PL-TR-93-2003

TGAL-93-01

STUDIES OF REGIONAL PHASE PROPAGATION IN EURASIA

Rong-Song Jih
Christopher S. Lynnes

Teledyne Geotech Alexandria Laboratory
314 Montgomery Street
Alexandria, VA 22314-1581

31 DECEMBER 1992

FINAL REPORT
16 August 1990 - 15 December 1992

APPROVED FOR PUBLIC RELEASE
DISTRIBUTION UNLIMITED

PHILLIPS LABORATORY
DIRECTORATE OF GEOPHYSICS
AIR FORCE MATERIEL COMMAND
HANSCOM AIR FORCE BASE, MASSACHUSETTS 01731-5000

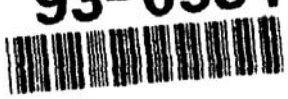

The views and conclusions contained in this document are those of the authors and should not be interpreted as representing the official policies, either expressed or implied, of the Air Force or the U.S. Government.

This technical report has been reviewed and is approved for publication.

JAMES F. LEWKOWICZ
Contract Manager
Solid Earth Geophysics Branch
Earth Sciences Division

JAMES F. LEWKOWICZ
Branch Chief
Solid Earth Geophysics Branch
Earth Sciencs Division

DONALD H. ECKHARDT, Director
Earth Sciences Division

This document has been reviewed by the ESD Public Affairs Office (PA) and is releasable to the National Technical Information Service (NTIS).

Qualified requestors may obtain additional copies from the Defense Technical Information Center. All others should apply to the National Technical Information Service.

If your address has changed, or if you wish to be removed from the mailing list, or if the addressee is no longer employed by your organization, please notify PL/IMA, Hanscom AFB MA 01731-5000. This will assist us in maintaining a current mailing list.

Do not return copies of this report unless contractual obligations or notices on a specific document requires that it be returned.

REPORT DOCUMENTATION PAGE

Form Approved
OMB No. 0704-0188

1. AGENCY USE ONLY (Leave blank)	2. REPORT DATE	3. REPORT TYPE AND DATES COVERED
	31 December 1992	Final Report, 16 Aug 1990 - 15 December 1992

4. TITLE AND SUBTITLE

Studies of Regional Phase Propagation in Eurasia

5. FUNDING NUMBERS

Contract F19628-90-C-0158

PE 62101F
PR 7600
TA 09
WU AT

6. AUTHOR(S)

R.-S. Jih and C. S. Lynnes*

7. PERFORMING ORGANIZATION NAME(S) AND ADDRESS(ES)

Teledyne Geotech Alexandria Laboratory
314 Montgomery Street
Alexandria, VA 22314-1581

8. PERFORMING ORGANIZATION REPORT NUMBER

TGAL-93-01

9. SPONSORING / MONITORING AGENCY NAME(S) AND ADDRESS(ES)

Phillips Laboratory
Hanscom AFB, MA 01731-5000
Contract Manager: J. Lewkowicz, PL/GPEH

10. SPONSORING / MONITORING AGENCY REPORT NUMBER

PL-TR-93-2003

11. SUPPLEMENTARY NOTES

*Hughes STX, 7601 Ora Glen Drive, Suite 300, Greenbelt, MD 20770

12a. DISTRIBUTION / AVAILABILITY STATEMENT

Approved for Public Release; Distribution Unlimited

12b. DISTRIBUTION CODE

13. ABSTRACT *(Maximum 200 words)*

We investigated various issues related to the propagation of seismic waves in Eurasia during the period 16 Aug 1990 - 15 Dec 1992. This final report covers the research accomplished under the 2 tasks that have not been reported previously in the first annual report *PL-TR-92-2042*.

Section I describes briefly how we derived a spherically symmetric velocity structure for the Garm region in Central Asia with travel-time residuals of regional phases recorded at the IRIS station GAR and and the CDSN station WMQ. In Section II, we conducted a tomographic inversion to determine the regional L_g Q structure in the Iranian Plateau. Although the whole of Iran can be regarded as a region of very low Q, applying a simple averaged attenuation coefficient (Q) for the whole plateau would be inappropriate for the L_g magnitude determination. The regional variation of the anelastic attenuation parameter is significant enough that it must be taken into account in calibrating each monitoring station for a reliable magnitude scale in monitoring possible clandestine tests from a vast area. Section III of this report gives a perspective overview of the whole project.

14. SUBJECT TERMS

Crustal Structure, Travel Time Inversion, Tomographic Inversion, L_g Attenuation, Crustal Phases, Magnitude Determination, Yield Estimation, Discrimination,

15. NUMBER OF PAGES

16. PRICE CODE

17. SECURITY CLASSIFICATION OF REPORT	18. SECURITY CLASSIFICATION OF THIS PAGE	19. SECURITY CLASSIFICATION OF ABSTRACT	20. LIMITATION OF ABSTRACT
Unclassified	Unclassified	Unclassified	UL

(THIS PAGE INTENTIONALLY LEFT BLANK)

SUMMARY

As part of Phillips Laboratory's **Eurasian Seismology Program**, we have been investigating the path effects on seismic waves under Contract **F19628-90-C-0158** during the period 16 Aug 1990 - 15 Dec 1992. Both theoretical and observational studies were conducted at different phases of this project to explore a wide spectrum of topics that are directly related to the monitoring of compliance of the Threshold Test Ban Treaty and the Non-Proliferation Treaty:

[1] Quantifying the path effects on body-wave amplitudes of Novaya Zemlya explosions.

[2] Preliminary yield estimates of Novaya Zemlya explosions with path-corrected m_b .

[3] ISC travel-time inversion in the Garm Region, Central Asia.

[4] Tomographic imaging of L_g Q structure in Iranian Plateau.

[5] Finite-difference modeling study of ripple-fired explosions.

[6] Preliminary yield estimate of Lop Nor explosion of 21 May 1992 based on a single-station observation.

The first two sections of this final report cover the research performed under Tasks 3 and 4, respectively. We present a perspective overview of the whole project in the third section, which also summarizes the work done under Tasks 5 and 6. The results obtained under Tasks 1 and 2 have been reported previously in our first annual report *PL-TR-92-2042.*

The objective of Task 3 is to obtain the velocity structure of the Garm region of Central Asia. Travel-time residuals of regional phases recorded at the IRIS station GAR and the CDSN station WMQ were used to derive a spherically symmetric structure for the crust and upper mantle in this region.

Under Task 4 we examined a general procedure which incorporates the independently derived information of localized path effects into the magnitude determination. The goal of this exercise is to quantify the bias in the seismic magnitude (such as $m_b(L_g)$) that would be inherent in a scheme without fully coupling the regional propagational characteristics into the magnitude determination procedure. Iran was chosen as a test case in this study because of the growing nuclear proliferation concern in the Middle East. A tentative zoning partitioning the Iranian Plateau into six regions has been used in our block inversion to reveal the spatial pattern of the L_g attenuation parameter, Q. Although the whole Iranian Plateau can be briefly described as a region of very low Q, applying a simple averaged attenuation coefficient (Q) for the whole plateau would be inappropriate for $m_b(L_g)$ calculation. The regional variation of the anelastic attenuation parameter is significant enough that it must be taken into account in calibrating each monitoring station for a reliable magnitude scale for monitoring possible clandestine tests from a vast area.

(THIS PAGE INTENTIONALLY LEFT BLANK)

Table of Contents

(THIS PAGE INTENTIONALLY LEFT BLANK)

SECTION I

TRAVEL TIME INVERSION IN THE GARM REGION

Christopher S. Lynnes[1] and Rong-Song Jih
Teledyne Geotech Alexandria laboratory
314 Montgomery Street
Alexandria, VA 22314

1. INTRODUCTION

The propagation of regional phases is still problematic: amplitudes and even the observability of phases can be highly variable. This has important implications for the application and efficacy of earthquake/explosion discriminants and event size estimation. At least some of this variation is likely due to the effects of lateral heterogeneity, particularly in the waveguides and near the boundaries along which regional phases such as P_g , P_n , S_n , and L_g propagate. The effects of lateral heterogeneity on regional phase propagation can be modeled using finite-difference methods. To employ these methods, however, a realistic velocity model is required. Block inversion of travel times is a well-established technique for deriving laterally heterogeneous velocity structures. In order to simplify the problem and improve ray coverage, a two-dimensional geometry is sought: the high seismicity rate in the vicinity of the IRIS station GAR provides such an opportunity. The first step in this process is the derivation of a spherically symmetric structure for the crust and upper mantle in this region. This model can then serve as the starting model for a two-dimensional velocity inversion in the vertical plane.

2. METHODOLOGY

The inversion method used herein is based on the joint inversion of hypocenters and velocity structure outlined by Crosson (1976). Beginning with a starting model, perturbations ($\Delta\mathbf{m}$) to the previous model $\mathbf{m}$ are sought to minimize the travel time residual vector $\mathbf{d} = \mathbf{T}^{\mathbf{pred}}-\mathbf{T}^{\mathbf{obs}}$. The model perturbations include both hypocentral parameters and velocity structure.

The above method requires computations of theoretical travel times, ray parameter and $\partial T/\partial z$ for all source-station pairs in an arbitrary velocity structure. As the solution of the two-

[1]Now with Hughes STX, 7601 Ora Glen Drive, Suite 300, Greenbelt, MD 20770.

point problem can be lengthy and unstable in the presence of low-velocity zones or strong gradients, we use Vidale's (1988) finite-difference technique to compute the travel times throughout a two-dimensional grid for a source at the surface. The various hypocentral partial derivatives are computed numerically, interpolating from the grid points at the corresponding focal depth and epicentral distance. Rays are also traced by following the travel time gradient back to the source at the surface in order to compute the velocity structure derivatives.

A joint hypocenter-structure inversion algorithm has been developed based on that described by Crosson (1976). Beginning with a starting model, perturbations (Δm_j) to the previous model m_j are sought to minimize the travel time residual vector $d_i = T_i^{pred} - T_i^{obs}$. The normal equations to be solved are $A_{ij}\,\Delta m_j = d_i$. For the hypocentral model parameters, the components of **A** are the partial derivatives of the predicted travel time for that event, assuming a flat earth:

$$T_x = -p\cos(\phi)$$

$$T_y = -p\sin(\phi)$$

$$T_z = \frac{\pm 1}{v_s\sqrt{1-(pv_s)^2}}$$

$$T_t = 1$$

where p is the ray parameter for a given source-station pair, ϕ is the source-station azimuth, and v_s is the velocity at the source. The earth structure parameters, which are defined in terms of slowness are simply given by:

$$\frac{\partial T}{\partial s_i} = \frac{h_i}{\sqrt{1-p^2 s_i^{-2}}}$$

where s_i is the slowness (v^{-1}) in layer i, and h_i is the thickness of layer i traversed by the ray. Similar equations can be obtained for a spherical earth.

The resulting matrix **A** for inverting p events and k layers is:

$$\begin{bmatrix} \mathbf{H}_1 & 0 & .. & 0 & \mathbf{S}_1 \\ 0 & \mathbf{H}_2 & .. & 0 & \mathbf{S}_2 \\ .. & .. & .. & .. & .. \\ 0 & 0 & .. & \mathbf{H}_p & \mathbf{S}_p \end{bmatrix}$$

where $\mathbf{H}_i$ is the hypocentral sub-matrix and $\mathbf{S}_i$ is the velocity structure sub-matrix for event i:

$$\mathbf{H}_i = \begin{bmatrix} T_{x_i1} & T_{y_i1} & T_{z_i1} & T_{t_i1} \\ T_{x_i2} & T_{y_i2} & T_{z_i2} & T_{t_i2} \\ .. & .. & .. & .. \\ T_{x_iN_i} & T_{y_iN_i} & T_{z_iN_i} & T_{t_iN_i} \end{bmatrix}$$

$$\mathbf{S}_i = \begin{bmatrix} T_{s_11} & T_{s_21} & .. & T_{s_k1} \\ T_{s_12} & T_{s_22} & .. & T_{s_k2} \\ .. & .. & .. & .. \\ T_{s_1N_i} & T_{s_2N_i} & .. & T_{s_kN_i} \end{bmatrix}$$

N_i is the number of observations for event i.

In reality, each row of **A** and **d** is weighted according to the precision and quality (impulsive or emergent) of the arrival time report contributing to **d**.

The equation $\mathbf{A}\Delta\mathbf{m} = \mathbf{d}$ is then solved for $\Delta\mathbf{m}$ by multiplying both sides by $\mathbf{A}^T$:

$$\mathbf{A}^T\mathbf{A}\ \Delta\mathbf{m} = \mathbf{A}^T\mathbf{d}$$

$$(\mathbf{A}^T\mathbf{A})^{-1}\ \mathbf{A}^T\mathbf{A}\ \Delta\mathbf{m} = (\mathbf{A}^T\mathbf{A})^{-1}\ \mathbf{A}^T\mathbf{d}$$

The matrix $\mathbf{A}^T\mathbf{A}$ is a sparse matrix of doubly-bordered block-diagonal form. The inversion thus lends itself well to conjugate gradient techniques, such as that described by Press *et al.* (1986). Unfortunately, the matrix $\mathbf{A}^T\mathbf{A}$ is often close to being singular, particularly since there are strong tradeoffs between the velocity in the source layer and the partial derivative with respect to depth. The near-singularity renders the matrix inversion unstable. To get around this problem, we decided to adopt the Sherman-Morrison inversion procedure (Press *et al.*, 1986), in which the matrix inverse is found for the purely block-diagonal matrix, and then successively modified for each row and column making up the borders. Increasing the number of events thus results in an increase of only order N^2 for the inversion of the normal equations.

In the actual joint inversion algorithm, the model perturbations are computed from inversion using a starting model, and are then added to the starting model. The procedure continues until model perturbations are sufficiently small for a given iteration, or the improvement of the travel time residual vector is sufficiently small. At each iteration, both the travel time and ray parameter must be recomputed for all source-station pairs for the current structure. In order to solve the two-point problem for a large number of pairs, we use Vidale's (1988)

algorithm for computing travel times everywhere within a grid using finite-difference. At each iteration, this grid need be computed only once for a source at the surface; travel times and ray parameters are then obtained from the grid point at the appropriate hypocentral depth and epicentral distance.

The implementation of the algorithm comprises three programs:

hvnormeqn:

constructs the normal equations.

hvinvert:

inverts for the solution, *i.e.*, the model perturbations.

hvadjust:

adds the model perturbations to the previous model.

This separation of the inversion program from the others allows us to vary parameters with each iteration, such as the damping added to the matrix $\mathbf{A}^T\mathbf{A}$, as well as to recover easily from inversion failures due to non-convergence of the conjugate gradient method. The joint inversion algorithm has been tested on synthetic cases and is now being applied to the ISC arrivals.

3. DATA AND RESULTS

Hypocenters and arrivals have been obtained from International Seismological Center (ISC) tapes for the years 1971-1982. They have been dearchived and reformatted for use by software for earth-structure inversion. The travel time data actually used in this study consist of those recorded at stations less than 1000 km (9°) away. The ISC locations (Figure 1) are used as the initial guesses for hypocentral parameters. Events were selected carefully to include close stations so that the tradeoff between depth, origin time and source layer velocity could be resolved.

Several studies (*e.g.*, Carter *et al.*, 1991) indicate the crust to be very thick in this region. Figure 2 shows reduced travel time residuals for events with ISC depths of 10-15 km. The travel time curve for the Soviet GAR model (which has a mantle velocity of about 8.22 km/s) is superimposed. The match is fairly good at this depth, with the thick crust confirmed by the large crustal-mantle phase crossover distance. Figure 3 shows the residuals for events with ISC depths between 40 and 45 km. The deterioration at depth may indicate that ISC depths are systematically overestimated due to the velocity model.

A starting model similar to the GAR model was used in the inversion. The mantle velocity was fixed at 8.2 km/s in order to stabilize the layer directly above. However, this velocity appears to be well constrained by the travel time slope from 400-1000 km (Figures 2-3). The crustal depth was fixed at 65 km. Figure 4 shows the results of the joint inversion. The resulting model is similar to the GAR model. The velocity gradient is slightly steeper in the upper crust. Below this is a 35-km thick lower crust of about 7 km/s, slightly lower than the GAR model velocity. The relocated depths are plotted against the ISC depths in Figure 5. As indicated in Figure 3, the relocated depths are generally less than the ISC depths.

4. CONCLUSIONS

A joint inversion algorithm for hypocenters and velocity structure has been developed based on the algorithm of Crosson (1976). Vidale's (1988) finite-difference travel time algorithm and the Sherman-Morrison inversion of sparse matrices have been used to speed execution for large numbers of events. A joint inversion for hypocenters and velocity structure in Central Asia yields a 1-dimensional model with a thick crust consisting a 30-km crust with a steep gradient and a roughly homogeneous 35-km lower crust of about 7 km/s. Focal depths appear to be systematically overestimated by the ISC. This model can be used as the starting model for a 2-dimensional tomographic inversion of a profile in central Asia.

5. ACKNOWLEDGES

This study was supported under Phillips Laboratory contracts F19628-90-C-0158. The views and conclusions contained in this paper are those of the authors and should not be interpreted as representing the official policies, either expressed or implied, of Hughes STX, Teledyne Inc., the U.S. Air Force or the U.S. Government.

6. REFERENCES

Carter, J., Coyne, J., Israelsson, H., Riviere-Barbier, F., Ryaboy, V., and A. Suteau-Henson (1991). Nuclear monitoring research at the Center for Seismic Studies, *Report PL-TR-91-2127,* Phillips Laboratory, Hanscom Air Force Base, MA. **(ADA239653)**

Crosson, R. S. (1976). Crustal structure modeling of earthquake data 1. Simultaneous least squares estimation of hypocenter and velocity parameters, *J. Geophys. Res.,* **81**, 3036-3046.

Given, J. W. and D. V. Helmberger (1980). Upper mantle structure of northwestern Eurasia, *J. Geophys. Res.,* **12**, 7183-7194.

Lees, J. M., and R. S. Crosson, 1989. Tomographic inversion for three-dimensional velocity structure at Mount St. Helens using earthquake data, *J. Geophys. Res.,* **94**, 5716-5728.

Press, W. H., Flannery, B. P., Teukolsky, S. A., and W. T. Vetterling, (1986). *Numerical Recipes,* New York: Cambridge University Press, 818 p.

Vidale, J. (1988). Finite-difference calculation of travel times, *Bull. Seism. Soc. Am.,* **78**, 2062-2076.

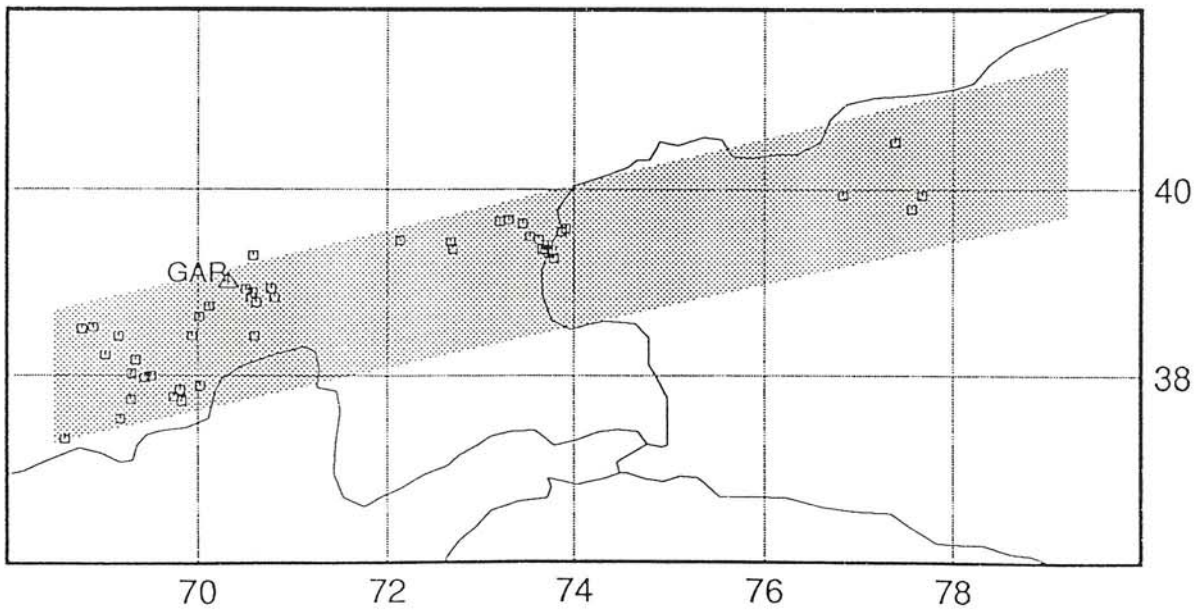

Figure 1. Index map showing the events used in the inversion, and station GAR.

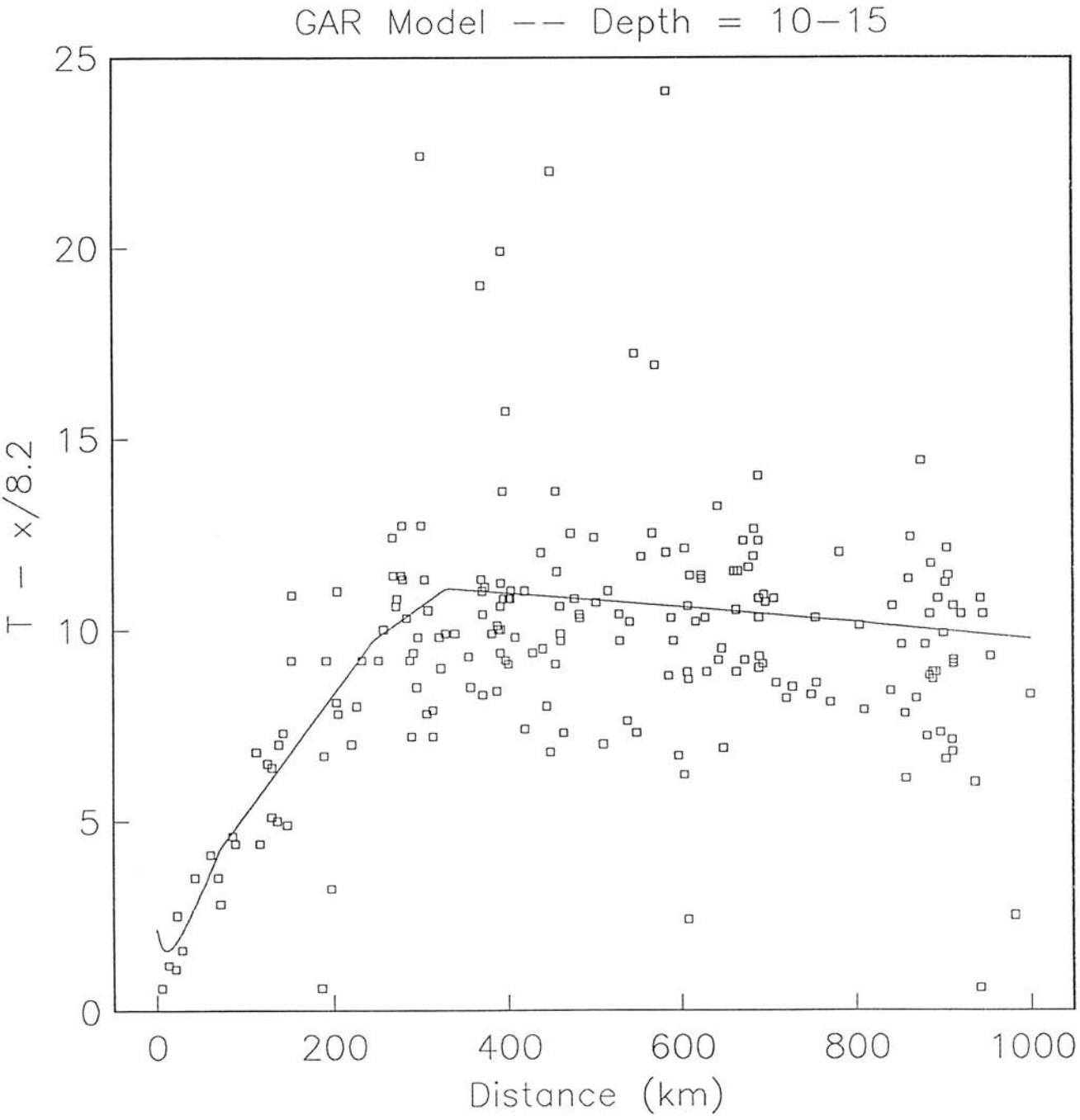

Figure 2. Reduced travel times for events 10-15 km in the shaded region of Figure 1 with ISC depths of 10-15 km. (The inversion events in this depth range are a subset of this set). The predicted travel time curve for the Soviet GAR model reported by Carter *et al.* (1991) is superimposed.

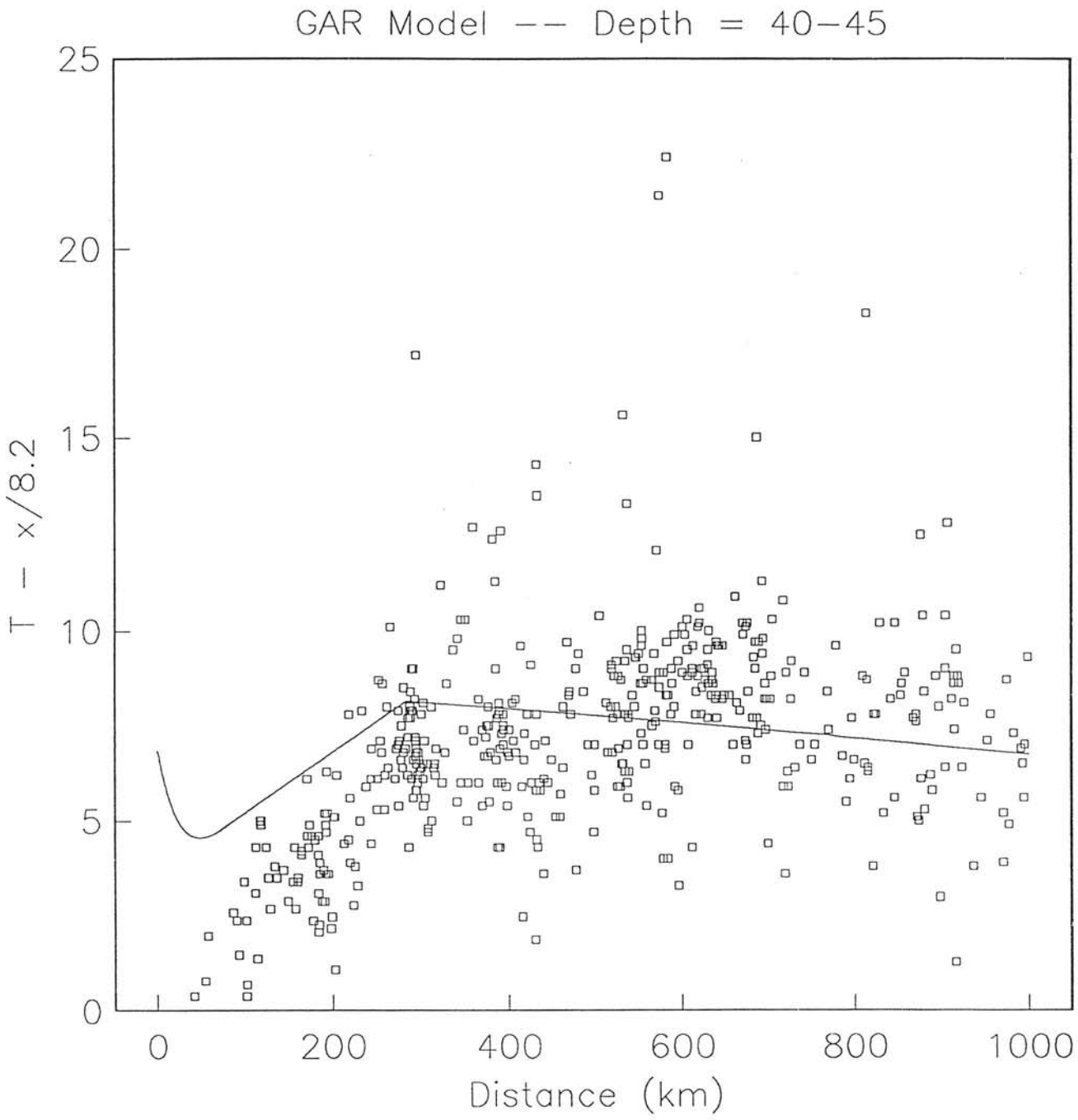

Figure 3. Same as Figure 2 for a depth range of 40-45 km. The small reduced travel times for close stations suggests the ISC depths are systematically overestimated.

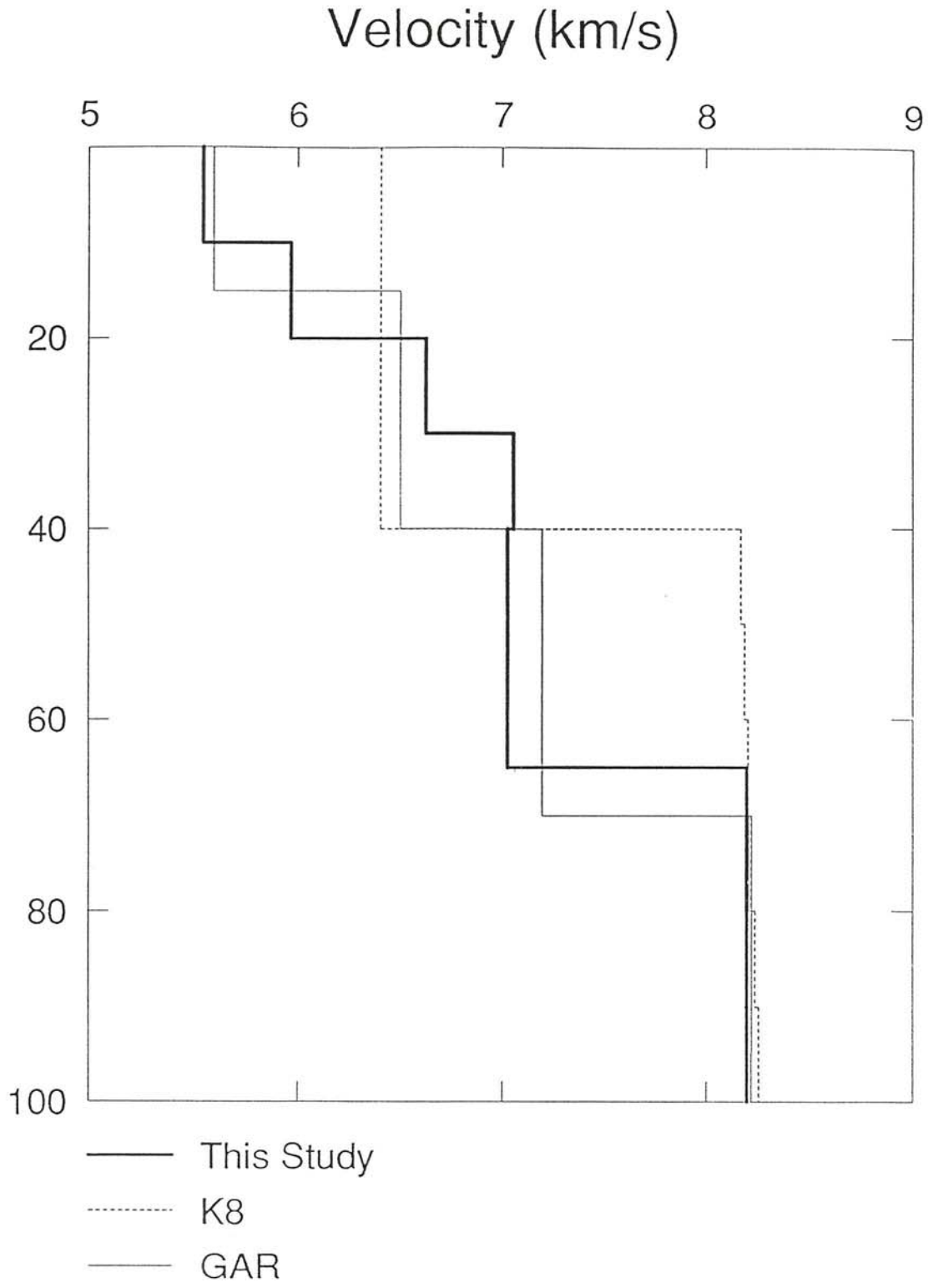

Figure 4. The final velocity model from the joint inversion is shown as the thick line. The Soviet model for station GAR (Carter *et al.*, 1991) and K8 model (Given and Helmberger, 1980) for NW Eurasia are shown for comparison.

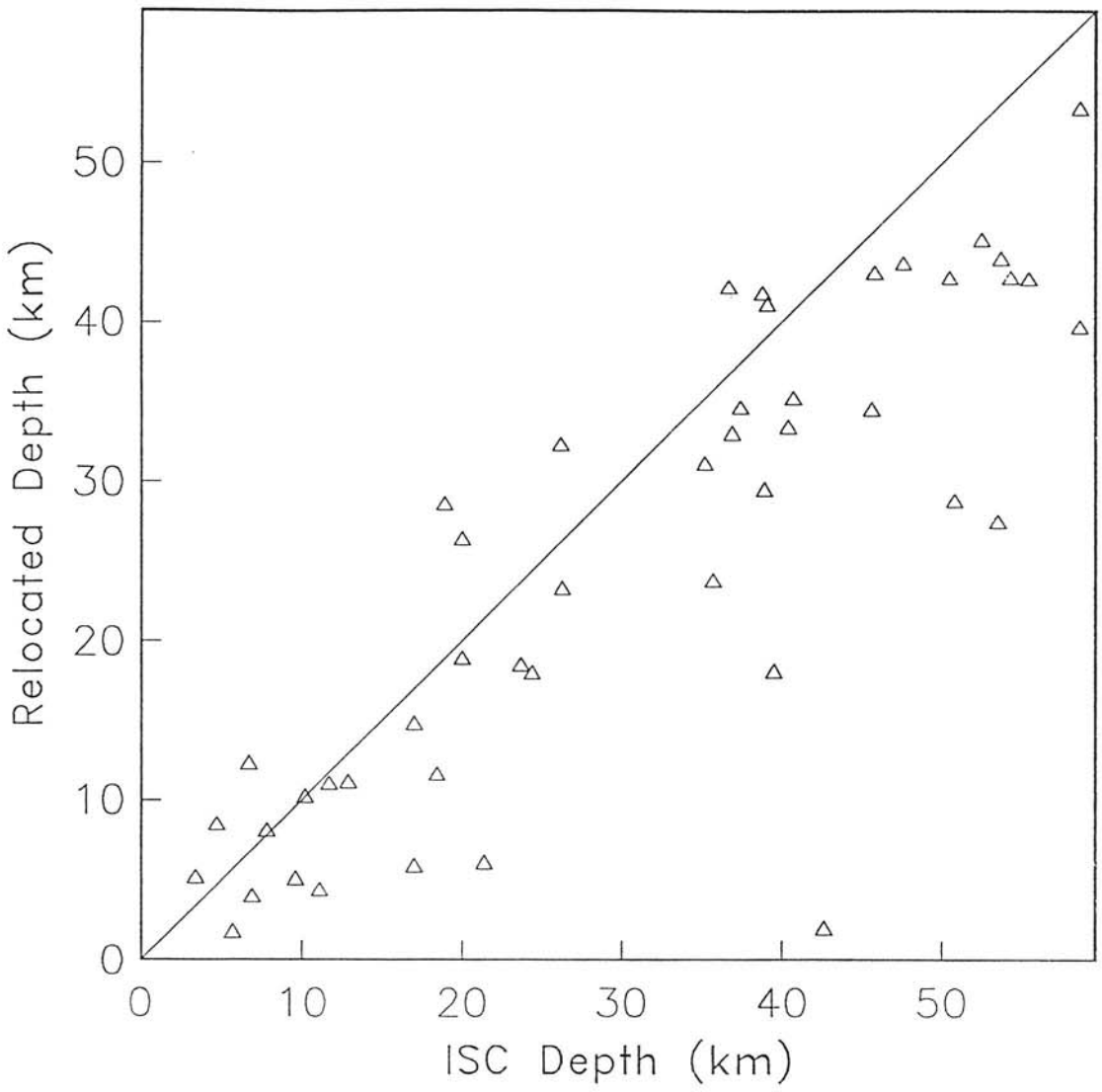

Figure 5. Hypocentral depths obtained from joint inversion plotted vs. those from the ISC. The inversion yields systematically shallower depths.

(THIS PAGE INTENTIONALLY LEFT BLANK)

Section II

REGIONAL L_g Q VARIATION IN IRANIAN PLATEAU AND ITS IMPLICATION FOR $m_b(L_g)$ DETERMINATION

Rong-Song Jih
Teledyne Geotech
314 Montgomery Street
Alexandria, VA 22314

Christopher S. Lynnes
Hughes STX
7601 Ora Glen Drive, Suite 300
Greenbelt, MD 20770

1. INTRODUCTION

An accurate characterization of the propagation of regional phases due to explosion sources in regions of high proliferation concern (such as Iran) requires fairly accurate crustal models. Iran lies on the Alpine-Himalayan seismo-tectonic belt, within a wide band of seismic activity connecting the Hindu Kush and eastern Mediterranean highly seismic regions. The Zagros Main Thrust Fault constitutes the boundary between the Iranian and Arabian Plates. Central Iran, northwest Iran, and the south Caspian areas have low levels of seismicity compared to those of the narrow belts surrounding them (McEvilly and Razani, 1971; Nowroozi, 1971, 1972, 1976; McKenzie, 1972; Dewey and Grantz, 1973; Hedayati *et al.*, 1976; Chandra *et al.*, 1979; Quinttmeyer and Jacob, 1979; Rowshandel *et al.*, 1981; Ambrasseys and Melville, 1982; Jackson and McKenzie, 1984, 1988; and many others). This is regarded as a highly heterogeneous and complicated geological environment (Leith, 1992).

The seismic structure of the Iranian Plateau has been discussed in several studies. For instance, using travel time residuals derived from data recorded at WWSSN stations in Iran (MSH, SHI, TAB), Chen *et al.* (1980) inferred an uppermost mantle *P*-wave velocity of 8.0±0.1 km/s for Iran. They also suggested that the crust dips toward the south-southeast at about 1°. Thus if the crustal thickness were 34 km in the north, it would reach about 49 km in the south. Kadinsky-Cade *et al.* (1981) also derived the average upper-mantle velocity beneath Iran with the same single-station method. Asudeh (1982) applied the two-station method to earthquakes along the interstation line, and he derived a *P*-wave velocity of 7.70±0.05 km/s with a crust 43 km thick between southern Iran and the SRO station MAIO. This profile crosses the Tabas area. Asudeh (1982) also derived simple velocity profiles for several other regions with MAIO and ILPA (Iranian Long Period Array) data. Asudeh (1982) suggests that the crust to the north, east, and central parts of the Iranian Plateau is approximately 10 km thicker than at its western extreme. Roughly, the crust thickens from SSW to

NNE across the Zagros Main Thrust Fault, contrary to the assertion made by Chen *et al.* (1980). Wallace's (1991) over-simplified two-block model of Iran seems to support Asudeh's (1982) interpretation. A point that should be made here is that, although a few crustal models have been proposed during the past three decades, the requirement to identify small seismic events has raised a need to refine the available crustal models for more detailed and more accurate regionalized profiles based on newly available data sources and methodologies.

This study covers two topics. In the first part, we establish a regionalized L_g Q map for Iranian Plateau with a 7-zone tomographic inversion. In the second part, we illustrate the importance of applying the 2-dimensional L_g Q map to $m_b(L_g)$ calculation. The bias in $m_b(L_g)$ due to erroneous constant Q model is quantified. Due to the preliminary nature of the result, however, it is not our intention to explain the cause of the regional variation of L_g Q in Iranian Plateau. Mitchell and Hwang (1987) find that the variation of L_g Q values between Applachian and Rocky Mountains can easily be produced by accumulations of sandstone and shale of Mesozoic age and younger. By contrast, throughout most of the Western United States, neither the low L_g Q values which have been observed nor the regional variation of those values can be explained by accumulation of low-Q sediments. Mitchell and Hwang (1987) suggest that the explanation requires low and laterally varying values of Q in the crystalline crust for Western United States. To explore the cause of the regional variation of L_g Q in Iranian Plateau would require more data and further investigation.

2. NUTTLI'S Lg ATTENUATION MEASUREMENTS

Nuttli (1980) selected 99 Iranian earthquakes which occurred during 1972-1974. For these earthquakes, the body-wave magnitude, m_b , varied from 3.7 to 6.0, with a median of 4.8, and the focal depth varied from 0 to 94 km, with a median of 43 km. Nuttli measured the γ of 109 paths recorded at three WWSSN [World Wide Standard Seismograph Network] stations in Iran: Mashad (MSH), Tabriz (TAB), and Shiraz (SHI). However, Nuttli (1980) did not tabulate the events he used. Instead of cross referencing the epicentral coordinates published in the *Bulletin of the International Seismological Centre,* we digitized Nuttli's hand-drawn maps to retrieve his epicenters. Figure 1 shows the re-constructed 109 L_g paths.

Nuttli (1980) measured the *"sustained maximum motion",* namely the amplitude equaled or exceeded by the three largest amplitude waves, of the vertical-component L_g waves with period around 1 second. A "normalized" amplitude, A^*, is defined as follows: the amplitude readings, $A(\Delta)$ (in μm), are first corrected for the effects of geometrical spreading and dispersion with the formula appropriate for an Airy phase (*cf.* Ewing *et al.*, 1957); then they are normalized according to Nuttli's empirical scaling that an Iranian event with ISC m_b 5.0 would have a hypothetical L_g amplitude of 270 μm at 10-km distance. All events are thus "equalized" to magnitude 5.0:

$$A^*(\Delta) \equiv A(\Delta) \cdot \Delta^{0.333} \cdot [\sin(\Delta/111.1)]^{0.5} \cdot 10^{3.6372 - m_b(ISC)} , \qquad [1]$$

If there is no anelastic attenuation or other scattering mechanism, the normalized amplitude, $A^*(\Delta)$, should be 1 at any distance, Δ. Otherwise, $A^*(\Delta)$ would be smaller than 1, and it is defined as $\exp[-\gamma(\Delta-10)]$, where γ is the anelastic absorption coefficient. When the normalized amplitudes $A^*(\Delta)$ are plotted as a function of Δ on a semi-logarithmic scale, the slope of the straight line connecting [10km, 0] and $[\Delta, \ln(A^*(\Delta))]$ would be exactly $-\gamma$. Nuttli used this time-domain approach to determine the attenuation coefficient, γ, of 109 paths in his study (*cf.* Figure 3 of Nuttli, 1980). The average γ of these 109 paths is 0.00442 km^{-1}, very close to that of 0.0048 for coastal California derived by Herrmann (1980). Solid and dashed lines in Figure 1 represent those paths with γ smaller and larger, respectively, than the average.

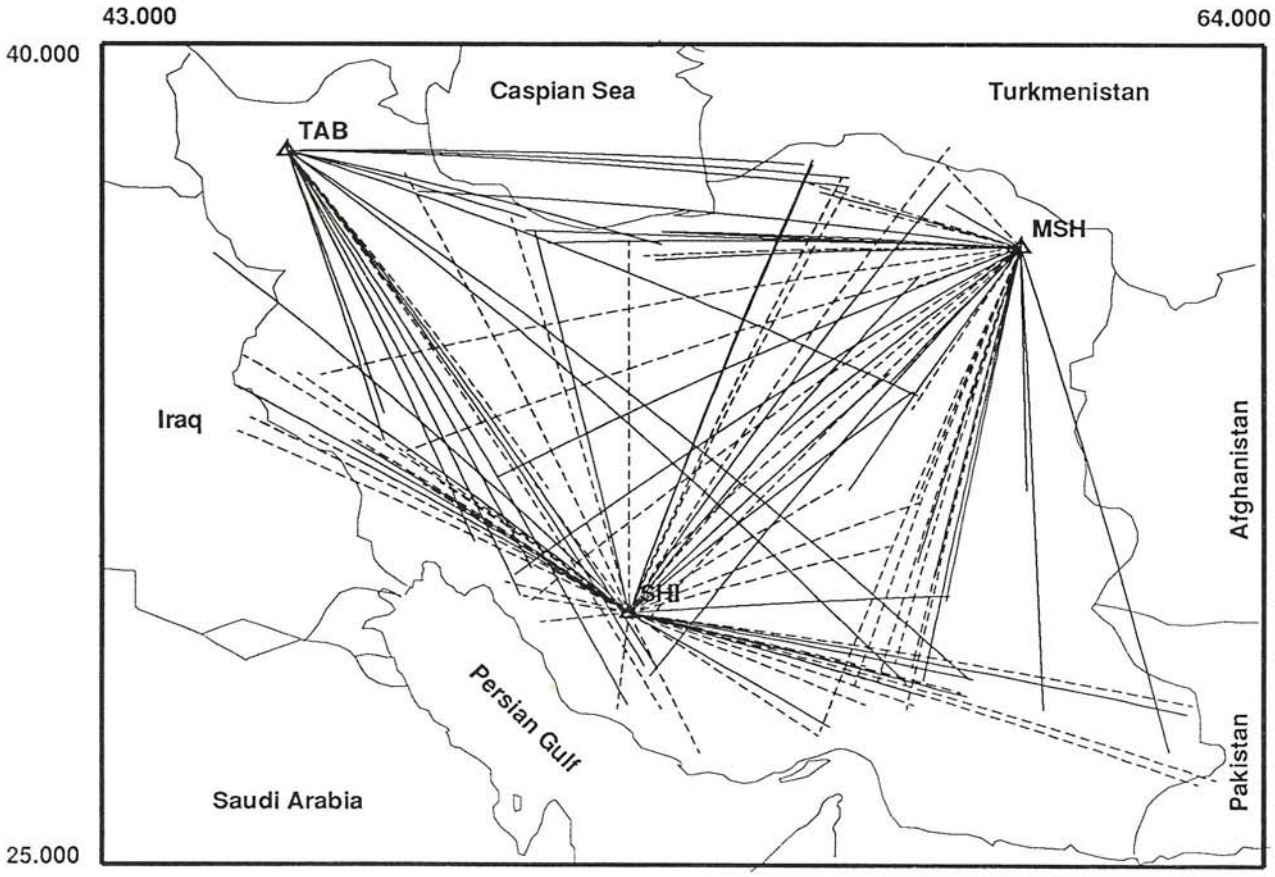

Figure 1. 109 L_g paths recorded at 3 WWSSN stations in Iran (MSH, TAB, and SHI) during 1972-1976 for which the attenuation parameter, γ, was readily measured by Nuttli (1980). Solid and dashed lines represent those with γ value smaller and larger than the average (0.0044 km^{-1}), respectively.

3. TOMOGRAPHIC IMAGING METHOD

The datum for seismic tomographic imaging is the integral of some physical parameter along a specified path through the medium. For example, the travel time accumulated along a ray path between a source and a receiver can be expressed as the integrated slowness; the amplitude decay can be expressed as the integrated attenuation. The application of tomographic imaging to construct the 2-dimensional map of lateral heterogeneity in the crust is essentially the same as the method that has been widely used for decades in X-ray tomography or radioastronomy.

Suppose there are M seismic sources recorded at some or all of N stations, and suppose that these events and stations are spread over K seismotectonic regions. For coding and computational simplicity, the region boundaries were chosen on a 0.333° by 0.333° grid. Thus each "seismotectonic province" is composed of many square cells of size 0.333° by 0.333°. We assume that the attenuation, γ_k, varies from one province (region) to another. The total path attenuation can be decomposed as the sum of the attenuation incurred in each region that the ray has traversed. That is,

$$\sum_{k=1}^{K} \gamma_k \, \Delta_k(i,j) = \gamma(i,j) \, \Delta(i,j) \ , \quad \text{for } i=1,\ldots, M \ ; \ j=1,\ldots, N \qquad [2]$$

where $\gamma(i,j)$ is the path attenuation that Nuttli (1980) already measured, and $\Delta(i,j)$ is that epicentral distance from the i'th event to the j'th station. On the left-hand side, γ_k is the (unknown) attenuation coefficient in the k'th region and $\Delta_k(i,j)$ is the distance traversed in the k'th region along the path from the i'th event to the j'th station. $\Delta_k(i,j)$ is computed as the sum of all segments of the great-circle path of the (i,j)'th ray that fall in a square cell comprising the k'th region. Thus $\Delta_k(i,j)$ would be 0 if the (i,j)'th ray does not cross any square cell of the k'th region. The determination of $\Delta_k(i, j)$ for i=1,...,M, j=1,...,N, is the crucial step of this linear tomographic imaging problem. Once the elements of matrix $[\Delta_k(i, j)]_{MxN}$ are known, it is straightforward to solve for the unknown vector, $[\gamma_1, \gamma_2, \ldots, \gamma_K]'$, with the standard least-squares techniques.

4. REGIONAL VARIATION OF Q IN IRANIAN PLATEAU

There have been different opinions regarding how Iranian Plateau should be partitioned in terms of the seismotectonic properties. Nowroozi (1976) presented 23 seismotectonic provinces for Iran based on 638 relocated earthquakes as well as 24 instrumentally located epicenters given by others. Berberian (1979) largely disagreed with the boundaries Nowroozi (1976) proposed, and he suggested that the only justifiable partitioning of the Iranian Plateau should be: [1] two Marginal Fold Belts of Zagros (in southwestern Iran) and Kopeh Dagh (in northeastern Iran) resting on the Arabian and Turan platforms, respectively; [2] the Central Iranian ranges and basins between them; and finally, [3] the post-colored melange-orhiolitic flysch belt of east and southeast Iran. Berberian's (1979) characterization of Iranian Plateau implies that some seismotectonic provinces in Nowroozi's (1976) map need to be merged.

If the ray paths sample each portion of the region of interest fairly well, then the tomographic imaging can be utilized to reveal the regional characteristics without the need to impose any specific *a priori* zoning. Thus the tomographic inversion technique can be used to test various hypotheses regarding the partitioning of Iran, whenever the data resolution permits. If, however, the data coverage is poor in a certain portion, as in the case of Nuttli's (1980) data set, then applying some regionalization based on the seismotectonic information is necessary and reasonable. Figure 2 shows a tentative regionalization which partitions Iran into 6 regions: Zagros Range, Lut Block, East Iran Range, Central Iran Range, Elburz/Caspian region, and Great Kavir/Esfaphan/Rezaiyeh.

The tomographic imaging result with this partitioning is listed in Table 1. East Iran Range and western Afghanistan have the poorest ray coverage in Nuttli's data set, and hence the uncertainty in the associated Q estimate is high. For other regions, the standard error in the Q value is around 10%. Both the Zagros Range and the Lut Block show a large γ of 0.005 km^{-1}, roughly corresponding to a Q of 181±12 and 183±18, respectively. The Kopet Dagh, Shahrud Doruneh, and the Qom region also seem to have a Q slightly smaller than the average. On the other hand, the Elburz Province and central Iran have a Q of about 250 for 1 Hz L_g waves, which may be the highest Q value in Iran. Despite the large uncertainty in the Q value for the western Afghanistan area, the estimated Q of 201 is in agreement with Nuttli's (1981) earlier work in which he pointed out that Afghanistan, northern Pakistan, and northern India have crustal Q values comparable to those of Iran and the western United States.

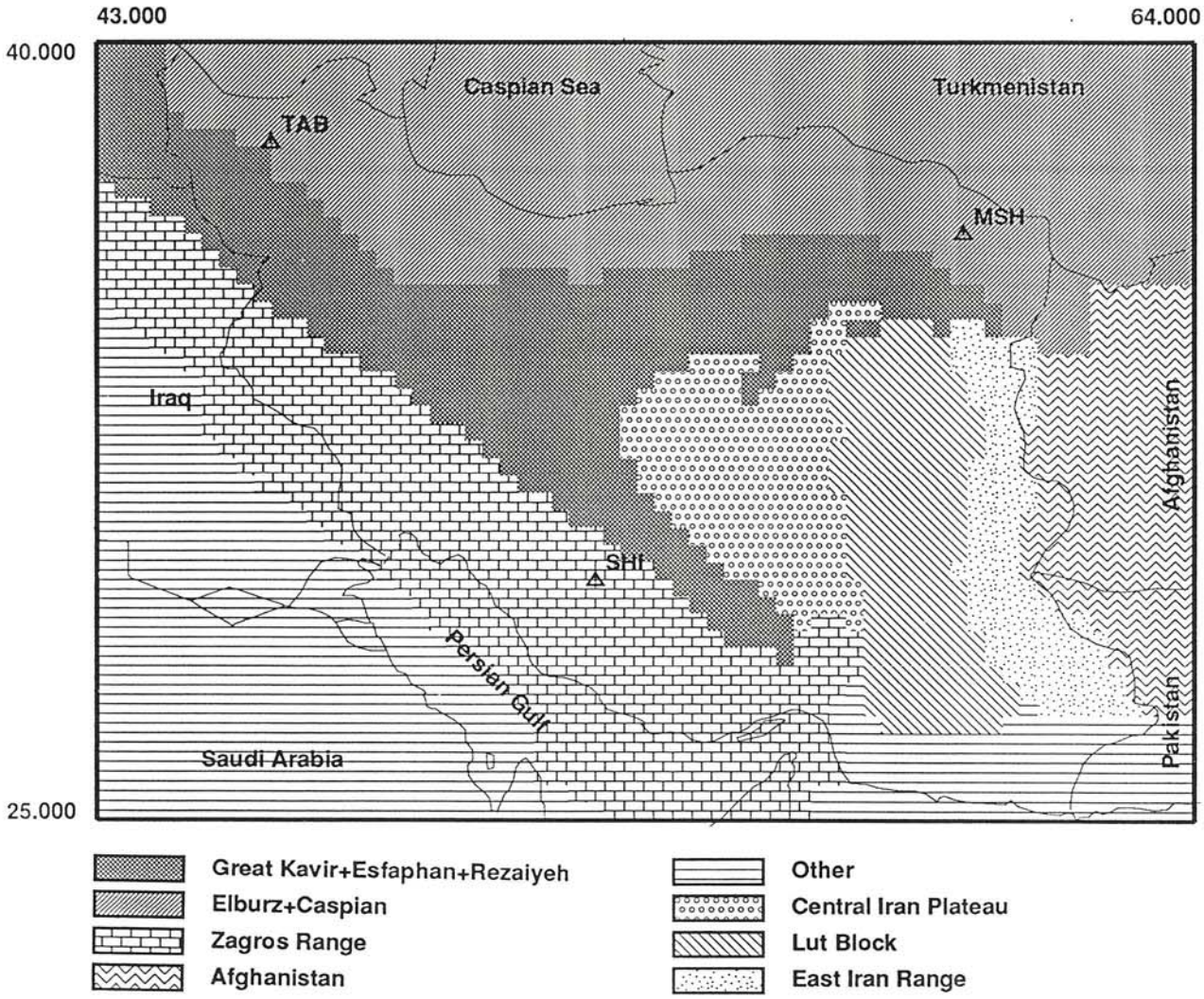

Figure 2. A preliminary regionalization which partitions Iran into 6 seismotectonic regions: Zagros Range, Lut Block, Eastern Iran Range, Central Iran Range, Elburz/Caspian region, and Great Kavir/Esfaphan/Rezaiyeh. Block inversion indicates that both the Zagros Range and the Lut Block show a large γ of 0.005 km^{-1}, roughly corresponding to a Q of 181±12 and 183±18, respectively. The Kopet Dagh, Shahrud Doruneh, and the Qom region also seem to have a Q slightly smaller than the average. The Elburz Province and central Iran have a Q of about 250 for 1 Hz L_g waves, which may be the highest Q value in Iran.

Table 1. Regional γ and Q of 1 Hz L_g in Iran

Region	γ (1/km)	Q_0
Central Iran Plateau	0.0037±0.0006	246±38
Elburz + Caspian	0.0035±0.0004	257±26
East Iran Range	0.0038±0.0013	248±91
Western Afghanistan	0.0045±0.0025	201±112
Great Kavir + Esfaphan + Rezaiyeh	0.0043±0.0003	209±16
Zagros Range	0.0049±0.0003	181±12
Lut Block	0.0049±0.0005	183±18

Table 2. Crustal Q Results of Various Regions*

Author	$Q_0 f^{\zeta}$	Geometrical Spreading + Dispersion	f (Hz)	Region	Method and Distance Range
Nuttli (1973)	1500	$\Delta^{-5/6}$	1	ENA	time domain amplitudes
Street (1976)	900	$\Delta^{-5/6}$	1	US & Canada E of Rockies	time domain amplitudes Δ ~ 200-4500 km
Horner et al. (1978)	1500	$\Delta^{-5/6}$	1	Canadian shield	time domain amplitudes Δ ~ 300-7000 km
Herrmann (1980)	229		1	Berkeley, CA	
Mechler et al. (1980)	400 $f^{0.44}$	$\Delta^{-5/6}$	0.5-8	France Δ = 350-1100 km	time domain max amps bandpass filtered data,
Mitchell (1981)	~900 $f^{0.2}$		0.25-1	ENA Δ = 500-2000 km	theoretical modeling of spectral shape
Nuttli (1981)	800 $f^{0.5}$ 1500 $f^{0.2}$		~1-5 "	ENA CUS	$\Delta \leq$ 1000 km
Nuttli (1981)	200 $f^{0.7}$		~1-5	S. Calif.	Lg coda, $\Delta \leq$ 1000 km
Dwyer et al. (1983)	1280 $f^{0.4}$	$\Delta^{-5/6}$	1-10	Central US	time domain max amps from bandpass filtered data, Δ = 200-2000 km

*) Partially adapted from Goncz et al. (1987).

Table 2. Crustal Q Results of Various Regions* (Continued)

Author	$Q_0 f^{\zeta}$	Geometrical Spreading + Dispersion	f (Hz)	Region	Method and Distance Range
Singh & Herrmann (1983)	$900 f^{0.35}$	$\Delta^{-5/6}$	0.5-3.5	NENA	Lg coda, 300-800 km
	$1000 f^{0.1}$	"	"	S. Appalachians	"
	$1200 f^{0.2}$	"	"	Central US	"
	$900 f^{0.25}$	"	"	Central Central US	"
Pulli (1984)	$660 f^{0.4}$		0.75-10	NENA	coda amps, ~ 50-600 km
Chen et al. (1984)	$(400\sim500) f^{0.0}$		~1	Beijing area	coda amps,
"	$(120\sim200) f^{0.2}$		~1	Yun-Nan, China	coda amps,
Raoof & Nuttli (1985)	$(130\sim350) f^{(0.4\sim0.7)}$	$\Delta^{-5/6}$	0.4-1.4	Andes	
"	$(420\sim580) f^{(0.2\sim0.3)}$	"	"	Patagonian	
"	$(580\sim980) f^{(0.0\sim0.2)}$	"	"	ESA	
Hasegawa (1985)	$900 f^{0.2}$	$\Delta^{-1/2}$	0.6-20	Canadian shield	spectra of ground accel. Δ ~ 70-900 km
Shin (1985)	$(500\pm50) f^{(0.6-0.7)}$	$\Delta^{-5/6}$	1-10	Eastern Canada	time domain max amps
"	$(500\pm50) f^{(0.6-0.7)}$	$\Delta^{-1/2}$	1-10	Eastern Canada	freq domain amp spectra Δ ~ 100-1000 km
Campillo et al. (1985)	$290 f^{0.52}$	$\Delta^{-5/6}$	0.5-10	France Δ = 150-2000 km	time domain max amps & theoretical modeling
Chavez & Priestley (1986)	$206 f^{0.68}$	$\Delta^{-1/2}$	0.3-10	US Great Basin explosions	frequency domain amps, Δ = 200-500 km
"	$214(\pm50) f^{0.54\pm0.09}$	"	0.3-5	US Great Basin earthquakes	"
Gupta & McLaughlin (1987)	$800 f^{0.32}$	$\Delta^{-5/6}$	0.5-7	EUS	amplitudes from PSRV Δ < 1100 km
	400 at 1 Hz	"	1	CUS	
	1100 at 1 Hz	"	"	EUS-CUS	
	1400 at 1 Hz	"	"	Appalachians	
Goncz et al. (1987)	$1000 f^{0.35}$	$\Delta^{-5/6}$	0.5-13	Central & ENA	time domain max amps Δ ~ 500-3000 km
Chun et al. (1987)	$1100 f^{0.19}$	$\Delta^{-1/2}$	0.6-10	Eastern Canada	spectral ratios Δ = 53-210 km
Xie & Mitchell (1990)	low	$\Delta^{-5/6}$		E. Africa Rift	
Chun et al. (1992)	$564(\pm53) f^{0.49\pm0.06}$	$\Delta^{-5/6}$	0.1-1.0	Asia	CDSN + IRIS
"	$283(\pm5) f^{0.72\pm0.02}$	"	0.3-3.5	Beijing area	$\Delta \leq$ 1000 km

*) Partially adapted from Goncz et al. (1987).

5. IMPLICATION FOR SEISMIC MONITORING

Attenuation of short-period L_g -wave motions is of concern for a number of seismological problems. For engineering purposes, L_g is often the wave group responsible for the largest and most prolonged ground motion observed on accelerograms, and hence it determines the "design motion" at a site. For seismicity studies, L_g amplitudes can be used to estimate 1-Hz m_b values for small earthquakes for which the P wave cannot be seen at teleseismic distances (Nuttli, 1973). For discrimination between earthquakes and explosions at regional distances, the ratio of L_g to P amplitudes has been investigated in many studies (*e.g.*, Blandford, 1981; Lynnes *et al.*, 1990; Lynnes and Baumstark, 1991).

For the purpose of calculating $m_b(L_g)$ in Iran, Nuttli's original L_g formula can be rewritten in an equivalent form:

$$m_b(L_g) \equiv 3.6372 + \log A(\Delta) + \frac{1}{3}\log(\Delta) + \frac{1}{2}\log\left[\sin\left(\frac{\Delta(\text{km})}{111.1(\text{km/deg})}\right)\right] + \frac{\gamma \cdot (\Delta - 10\text{km})}{\ln(10)}, \quad [3]$$

$$\text{where } \gamma \equiv \frac{\pi}{Q \cdot U \cdot T}, \qquad Q(f) = Q_0 \cdot f^{\zeta},$$

Δ is the epicentral distance in km, $A(\Delta)$ is the observed L_g amplitude measured in the time domain in μm [microns] at the epicentral distance of Δ km. For instance, a seismic source in Iran with 1-sec L_g amplitude of 270 μm at 10 km epicentral distance would correspond to a $m_b(L_g)$ of 3.6372 + 2.4314 + 0.3333 - 1.4019 + 0.0000 = 5.000, same as what Nuttli's (1986) formula would give. Nuttli's (1986) later study of L_g suggested that a different constant of 4.0272 is required for Eastern North America and Central Asia regions (Jih, 1992). The bias of 0.39 m.u. could reflect the difference in L_g excitation relative to m_b (ISC) between Eastern U.S. (or Central Asia) and Iran. Alternatively, it could reflect the m_b bias between these two areas. This issue will be discussed later.

Once the regionalized γ map is available, an individual path γ for an arbitrary source-station pair can simply be computed as the weighted sum of the γ_k's of the subregions that the ray path traverses:

$$\gamma = \sum_{k=1}^{K} \gamma_k \cdot \frac{\Delta_k}{\Delta}, \quad [4]$$

It is clear from [3] that an erroneous path γ would yield a $m_b(L_g)$ bias which increases with the distance. Furthermore, this error is independent of the actual source size or the quality of the amplitude measured at the recording station. It is *the bias* solely due to inaccurate calibration of the propagation effect.

Figure 3 shows the spatial pattern of apparent $m_b(L_g)$ corrections that would be needed at WWSSN station SHI and IRIS station ASH (Ashkhabad), respectively, if a constant γ of 0.0044 km^{-1} (*viz.*, the average γ across Iran) was assumed in computing $m_b(L_g)$ at these two stations. For each hypothetical epicenter, the $m_b(L_g)$ correction required is independent of the amplitude actually observed (*cf.* Equation [3]).

Partitioning Iran into 21 regions as proposed by Nowroozi (1976) (Figure 4) in our block inversion would yield more prominent spatial variations in the resulting Q map (Figure 5), and hence a stronger variation in $m_b(L_g)$ residual as well. The regional variation of the anelastic attenuation parameter in Figure 5 is significant enough that it needs to be taken into account in calibrating each monitoring station for a reliable magnitude scale in monitoring possible clandestine tests from a vast area. Unless this has been done, adding more stations/arrays to the monitoring network may not provide substantial improvement in reducing the error in the network-averaged magnitude based on regional phases. In fact, since the bias increases with distance, the bias in $m_b(L_g)$ would be much smaller if the magnitude were based on the nearest station alone (as compared to using a network of sparse stations for simple averaging). Figure 6 shows the spatial pattern of apparent $m_b(L_g)$ corrections as a function of hypothetical hypocenters that would be needed for a network of 3 stations (SHI, TAB, and MSH) if a constant γ of 0.0044 km^{-1} were assumed in computing $m_b(L_g)$ at these three stations. The residuals are determined with respect to 7- (top) and 21-zone (bottom) tomographic inversions, respectively. Note that magnitudes based on the network average is not necessarily better than those based on the nearest station alone, if the path attenuation is not carefully accounted for. This should be obvious by comparing Figures 3 and 6.

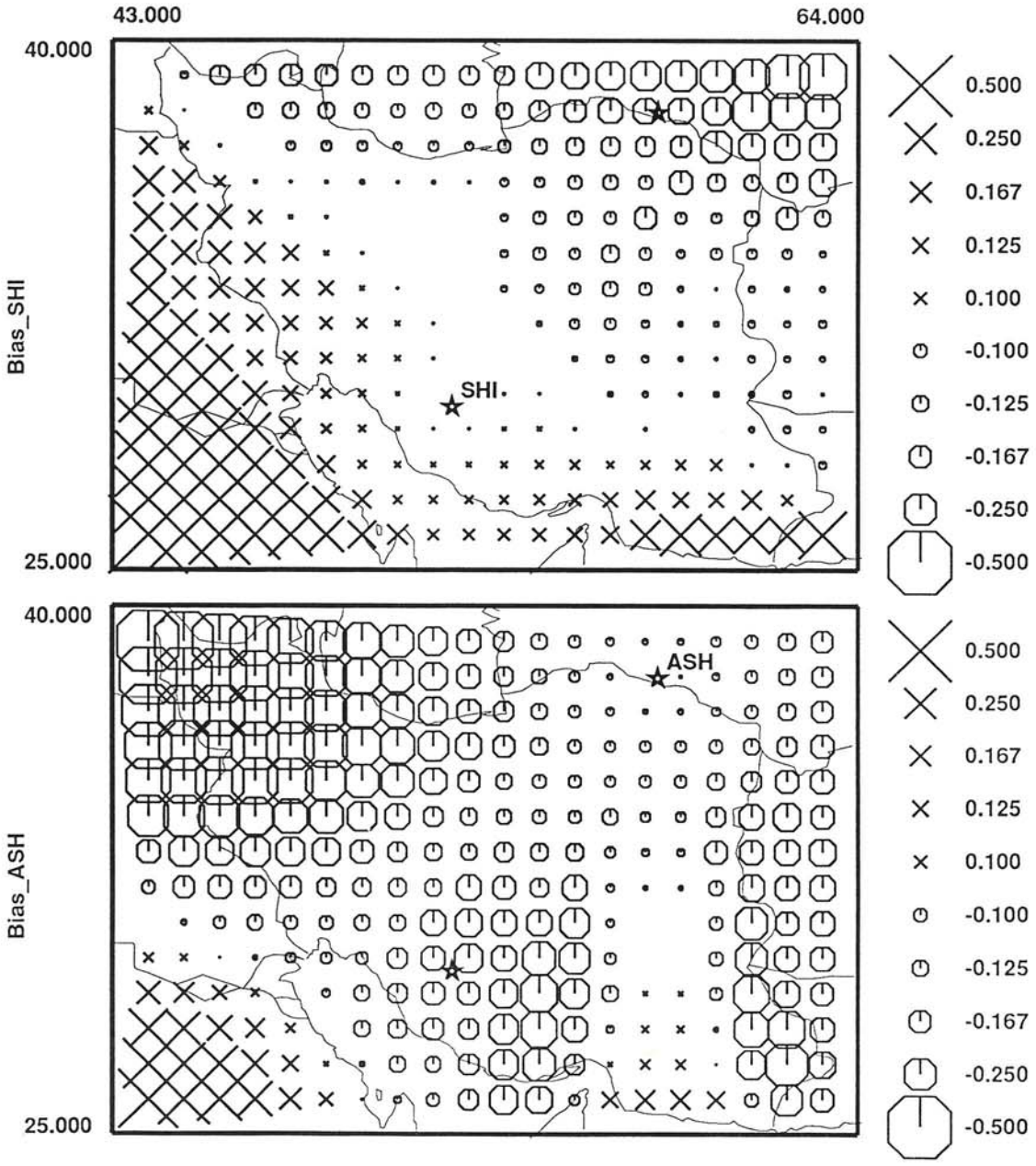

Figure 3. The spatial pattern of apparent $m_b(L_g)$ corrections as a function of hypothetical hypocenters that would be needed at WWSSN station SHI (top) and IRIS station ASH (bottom) if a constant γ of 0.0044 km^{-1} (viz, the average γ across Iran) were assumed in computing $m_b(L_g)$ at these two stations.

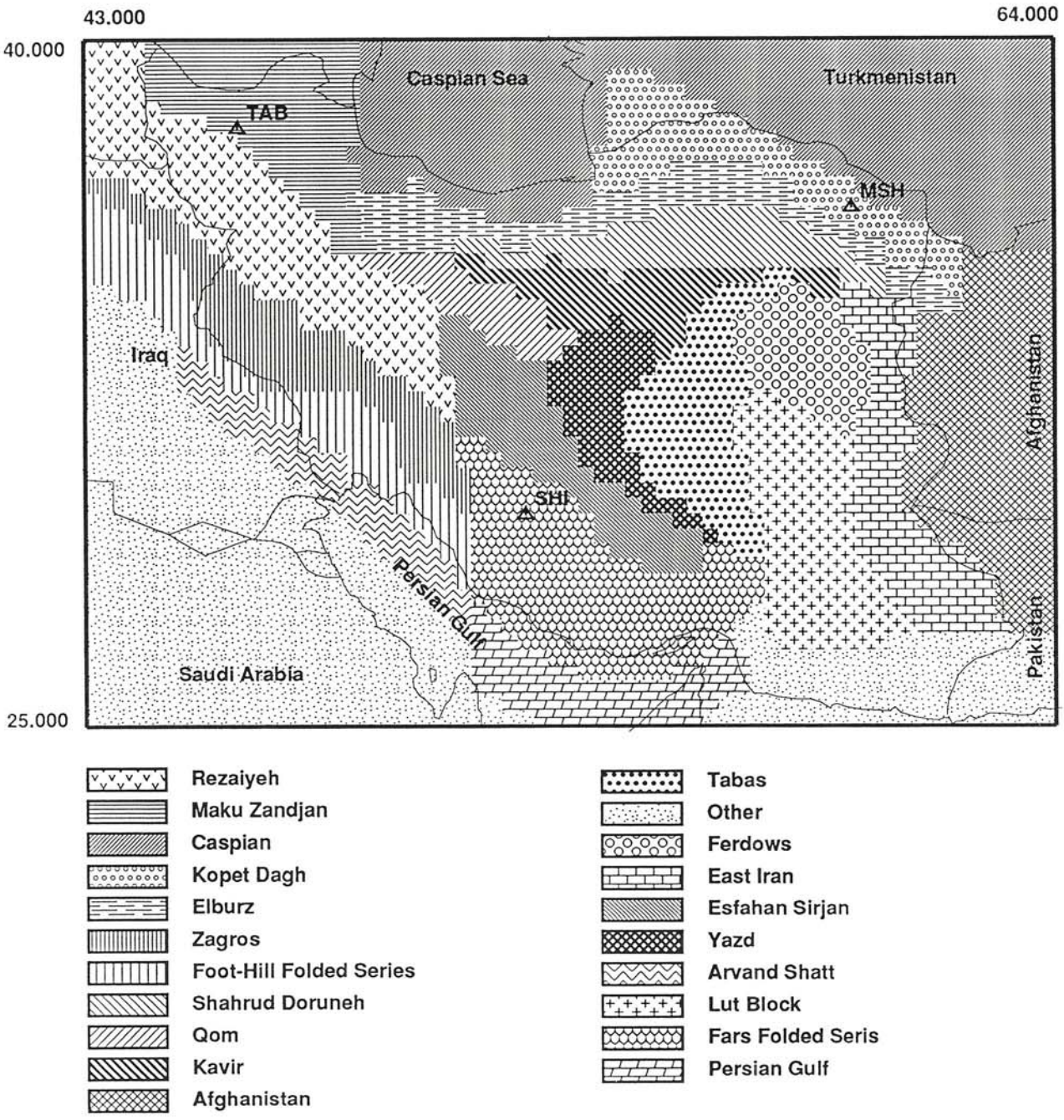

Figure 4. A more detailed partitioning of Iran as proposed by Nowroozi (1976) which partitions Iran into 21 regions.

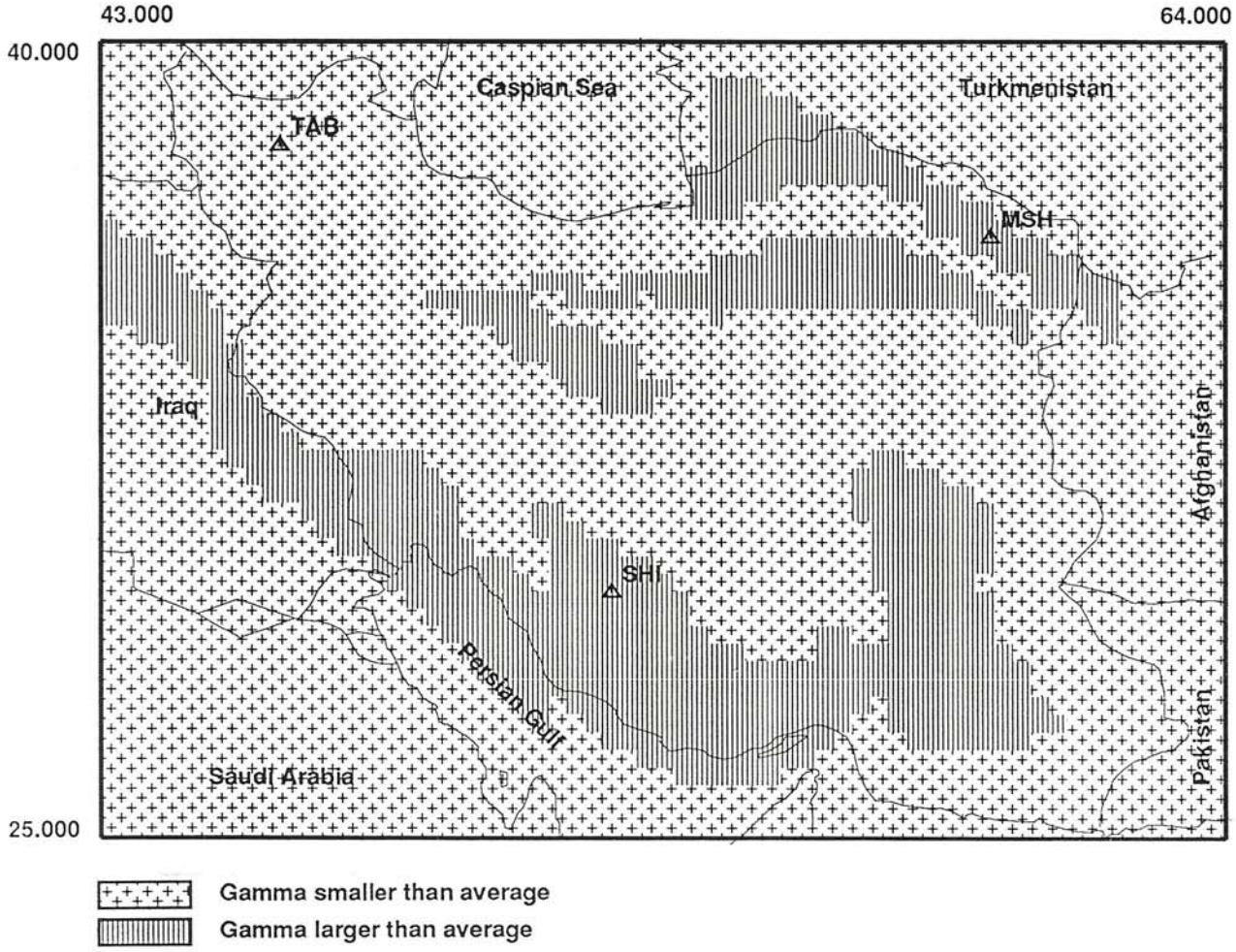

Figure 5. Partitioning Iran into 21 regions as proposed by Nowroozi (1976) in our block inversion would yield more prominent spatial variations in the resulting Q map as well as a more complicated pattern of $m_b(L_g)$ residual.

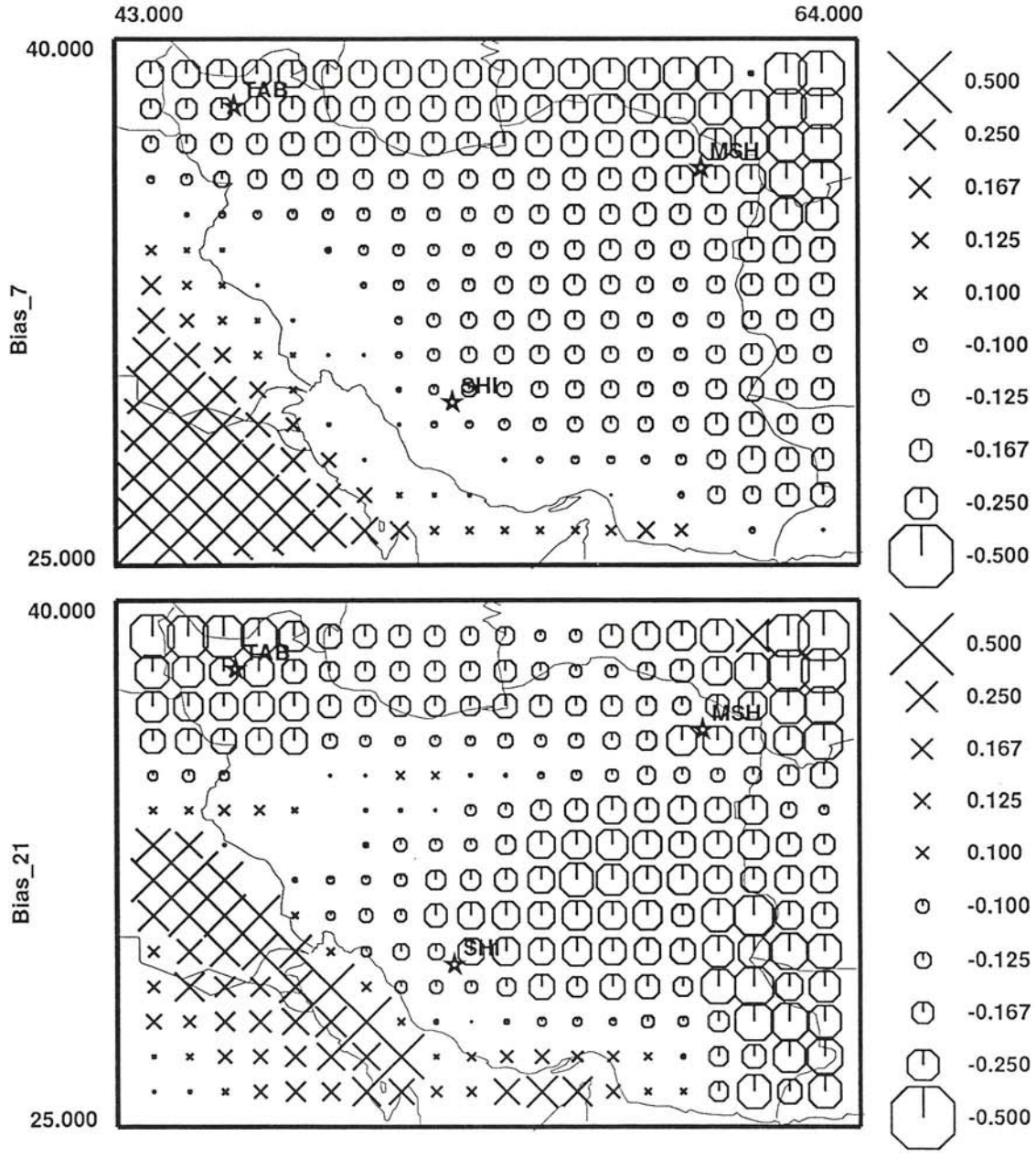

Figure 6. The spatial pattern of apparent $m_b(L_g)$ corrections as a function of hypothetical hypocenters that would be needed for a network of 3 stations (SHI, TAB, and MSH) if a constant γ of 0.0044 km^{-1} were assumed in computing $m_b(L_g)$ at these three stations. Top and bottom show the results of 7- and 21-zone tomographic inversion, respectively. Magnitude based on the network average is not necessarily better than that based on the nearest station alone, if the path attenuation is not carefully accounted for.

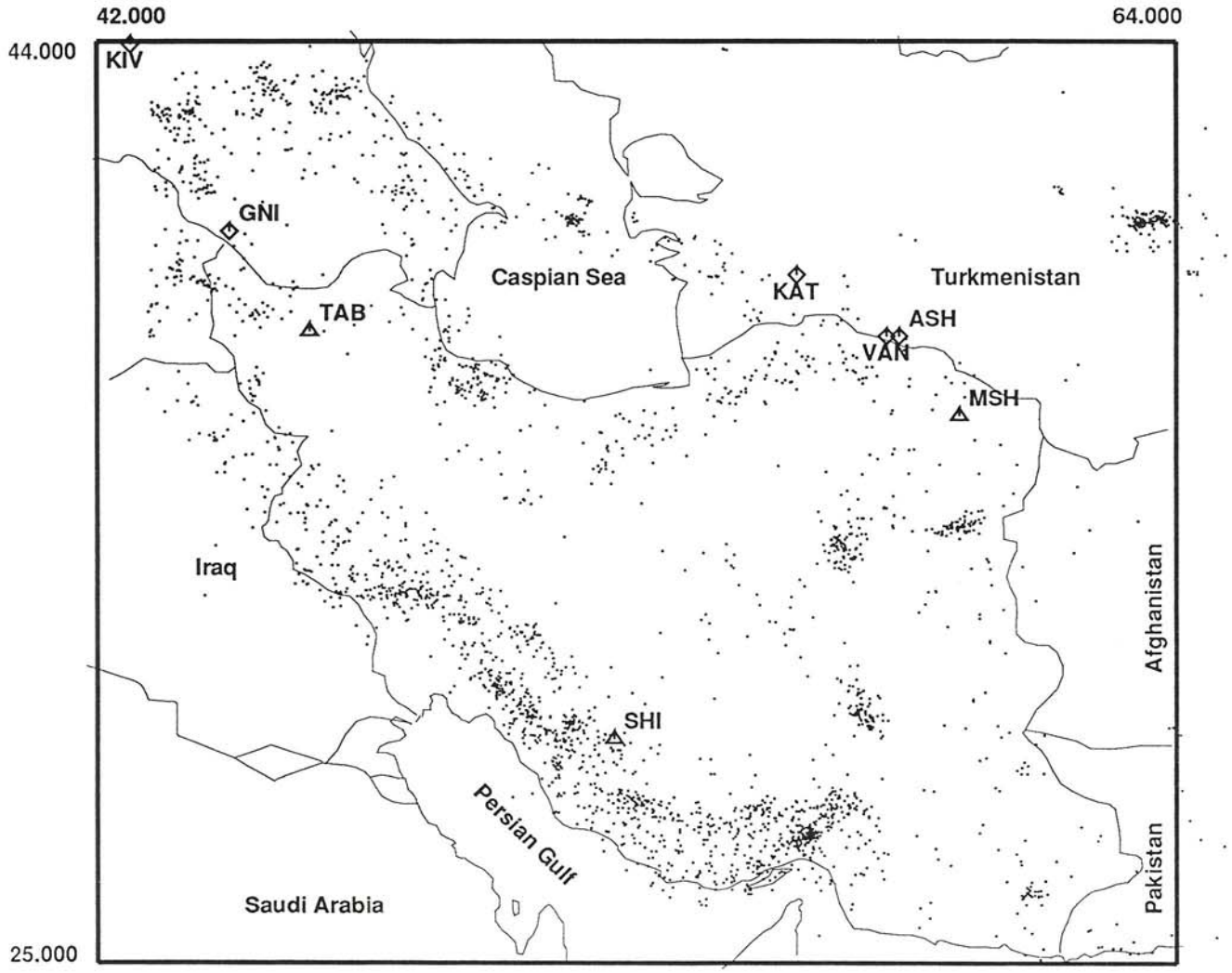

Figure 7. The seismicity map of Iranian Plateau showing all events with $m_b > 4$.

6. CONCLUSION

Although the whole Iranian Plateau can be briefly described as a region of very low Q, applying a simple averaged attenuation coefficient (Q) for the whole plateau would be inappropriate for measuring $m_b(L_g)$. The regional variation of the anelastic attenuation parameter is significant enough that it needs to be taken into account in calibrating each monitoring station for a reliable magnitude scale in monitoring possible clandestine tests from a vast area. Unless this has been done, adding more stations/arrays to the monitoring network may not provide substantial improvement in reducing the error in the network-averaged magnitude based on regional phases. In fact, since the bias increases with distance, the bias in $m_b(L_g)$ would be much smaller if the magnitude were based on the nearest station alone (as compared to using a network of sparse stations for simple averaging). This situation may be very different from that of monitoring a specific nuclear test site for which the empirical site-dependent correction term can be applied afterwards to the station magnitudes even when the path Qs are not fully known beforehand. For istance, Jih (1992) recently demonstrated a joint inversion procedure which can determine the L_g -based explosion size estimate as well as the path attenuation coefficient simultaneously. Such a technique would be most useful for calibrating the regions where underground nuclear tests or other man-made seismic events frequently take place. For regions like Iran where relatively very little is known about what the explosion signature should look like, however, a regionalized γ map (*e.g.*, Singh and Herrmann, 1983, for North America; and that in Kadinsky-Cade *et al.*, 1982, for S_n) for each crustal phase of interest should be established and applied to the routine magnitude computation procedure.

7. RECOMMENDATIONS

Nuttli (1980) suggested that a seismic source in Iran with the ISC bulletin m_b 5.0 should excite L_g amplitude of 270 microns at a 10-km extrapolated distance, whereas the seismic sources in Central Asia and eastern North America with comparable ISC bulletin m_b would excite a L_g amplitude of 110~150 microns (Nuttli, 1986). Possible explanations for this apparent bias of 0.26~0.39 m.u. include [1] uncertainty in the ISC bulletin m_b values (Nuttli, 1981), [2] differences in L_g excitation relative to m_b, or [3] differences in the upper mantle property which could cause a bias in m_b. Many L_g studies have used the ISC m_b for "normalizing" their L_g magnitude scale (*e.g.*, page 2146 of Nuttli, 1986a; page 128 of Israelson, 1992). Without careful re-processing, the ISC bulletin m_b values typically would be associated with large uncertainty. Therefore, it is very important to adopt a better m_b in calibrating

the crustal phases in Iran (or any other area of proliferation concern) in the first place. Magnitudes based on the short-period teleseismic recordings corrected for the station amplifications as well as the path effects (due to the focusing/defocusing near the source region *etc.*) such as those in Jih and Wagner (1992ab) may better serve such a purpose.

Wallace (1991) reports that the central Iran region has more efficient L_g propagation than the surrounding area, qualitatively in agreement with our result in Table 1. Many previous studies (*e.g.*, Ruzaikan *et al.*, 1977; Kadinsky-Cade *et al.*, 1981; Ni and Barazangi, 1982; Pomeroy *et al.*, 1982; Wallace, 1991) have pointed out that L_g, S_n, and P_n do not necessarily have the same propagation characteristics. For instance, the inefficient S_n propagation beneath the northern Iranian Plateau identified by Kadinsky-Cade *et al.* (1981) seems to permit efficient L_g propagation (Figure 6). The spectral and phase discrimination methodologies should take this into account. A regionalized γ map (*e.g.*, Figure 5 for L_g in Iran; the map derived by Singh and Herrmann, 1983, for North America; and that in Kadinsky-Cade *et al.*, 1982, for S_n) for each crustal phase of interest should be established and applied to the routine magnitude computation procedure such as the one in the knowledge-based automatic processing system (Bratt *et al.*, 1991).

Fault-plane solutions for many suitably located earthquakes in the Middle East have been determined by McKenzie (1972) and Jackson and McKenzie (1984). We recommend assembling events recorded at regional as well as at teleseismic distances according to the clustering of earthquakes with similar focal mechanism. Preferably for each crustal phase at least 10 events in each clustered area (*cf.* Figure 7) should be measured. The redundancy of data in each group will provide better constraints for inferring the empirical station and region-specific path corrections (Jih and Wagner, 1992ab; Jih, 1992), and it will thereby result in more precise magnitude scales for both regional and teleseismic phases. The determination of seismic magnitudes for events occurring in isolated suspected spots will also benefit from this exercise significantly, since more accurate station corrections will be available. Although several crustal models of the Middle East have been suggested during the past three decades, the task of identifying small seismic events requires a refinement of the available models for more detailed and more accurate regionalized profiles. Consequently, more tomographic inversions of the Middle East would be very useful.

To be more specific, we recommend first to assemble broadband digital data of recent seismic events of Iran (and Iraq) recorded at IRIS stations/arrays (ASH, KIV, and GNI) and then to complement this data set with digital data of MAIO (SRO) and analog recordings of historical events recorded at WWSSN and other former Soviet stations nearby. We suggest

that phase parameters of L_g, Rayleigh waves, and other regional phases be measured, and then inverted for the regionalized anelastic attenuation coefficients as well as for the crustal structures of Iran (and Iraq). Our preliminary result along these lines as presented in this study can be improved further by using an enlarged data set along with a more carefully defined seismotectonic map. We recommend that the m_b (of relatively larger events) and $m_b(L_g)$ be determined with two simultaneous inversion procedures which have been tested with Soviet events (Jih and Wagner, 1992ab; Jih, 1992). The resulting refined m_b values should then be applied to normalize the regional and local magnitudes of Iranian events. More detailed phase discrimination studies, such as those in Lynnes and Baumstark (1991) and Lynnes *et al.* (1990), should be conducted for the Iranian region with the improved phase parameters to be obtained in the manner we suggest.

8. ACKNOWLEDGEMENTS

The authors wish they could express their gratitude to the late Otto W. Nuttli of Saint Louis University. Discussions with Robert Blandford, Anton Dainty, Alan Ryall, Dave Russel, and Howard Patton have been very helpful. Wilmer Rivers and Peter Davis reviewed and improved the manuscript. The PSLIB plotting library released by Paul Wessel (HIG) and Walter Smith (Scripps) has been used in preparing some of the figures. Andy and Allen Jih (then 2nd and 4th graders, respectively) assisted the digitization of the epicenters of Nuttli's data set. This study was jointly supported under Phillips Laboratory contracts F19628-90-C-0158 and F29601-91-C-DB23, with part of the tomography code developed in 1986 under a previous DARPA contract F19628-85-C-0054 monitored by Air Force Geophysics Laboratory (now Phillips Laboratory). The views and conclusions contained in this paper are those of the authors and should not be interpreted as representing the official policies, either expressed or implied, of Teledyne Inc., Hughes STX, the U.S. Air Force, Defense Advanced Research Project Agency or the U.S. Government.

9. REFERENCES

Aki, K., A. Christoffersson, and E. S. Huesbye (1977). Determination of the three-dimensional seismic structure of the lithosphere, *J. Geophys. Res.*, **82,** 277-296.

Ambraseys, N. N. and C. P. Melville (1982). *A History of Persian Earthquakes,* University Press, Cambridge, U.K., 219 pages.

Asudeh, I. (1982). Seismic structure of Iran from surface and body wave data, *Geophys. J. R. astr. Soc.*, **71,** 715-730.

Berberian, M. (1979). Discussion of the paper *"Seismotectonic provinces of Iran"* by A. A. Nowroozi, *Bull. Seism. Soc. Am.*, **69,** 293-297.

Blandford, R. R. (1981). Seismic discrimination problems at regional distances, in *Identification of Seismic Sources - Earthquake or Underground Explosion,* (E. S. Husebye and S. Mykkeltveit, eds.), D. Reidel Publishing Co., Dordrecht, The Netherlands, 695-740.

Bollinger, G. A. (1979). Attenuation of the L_g phase and the determination of m_b in the Southeastern United States, *Bull. Seism. Soc. Am.*, **69,** 45-63.

Bratt, S. R., G. W. Beall, H. J. Swanger, F. K. Dashiell, and T. C. Bache (1991). A knowledge-based system for automatic interpretation of seismic data to associate signals and locate events, *NMRD Quarterly Report #8, SAIC-91/1281,* Science Applications International, San Diego, CA.

Bucher, R. L. and R. B. Smith (1971). Crustal structure of the eastern Basin and Range province and the northern Colorado Plateau from phase velocities of Rayleigh waves, in *Geophys. Mono. 14, The Structure and Physical Properties of the Earth's Crust,* 57-70, A.G.U., Washington, D.C.

Campillo, M., M. Bouchon, and B. Massinon (1984). Theoretical study of the excitation, spectral characteristics, and geometrical attenuation of regional seismic phases, *Bull. Seism. Soc. Am. 74,* 79-90.

Campillo, M., J. Plantet, M. Bouchon (1985). Frequency dependent attenuation in the crust beneath central France from L_g waves: data analysis and numerical modeling. *Bull. Seism. Soc. Am.*, **75,** 1395-1411.

Chandra, U., J. G. McWhorter, and A. A. Nowroozi (1979). Attenuation of intensities in Iran, *Bull. Seism. Soc. Am.*, **69,** 237-250.

Chavez, D. E. and K. F. Priestly (1986). Measurement of frequency dependent L_g attenuation in the Great Basin, *Geophys. Res. Let.*, **13,** 551-554.

Chen, C.-Y., W.-P., Chen, and P. Molnar (1980). The uppermost mantle $P-$wave velocities beneath Turkey and Iran, *Geophys. Res. Lett.*, **7,** 77-80.

Chen, P., O. W. Nuttli, W. Ye, and J. Qin (1984). Eatimates of short-period Q values and seismic moments from coda waves for earthquakes of the Beijing and Yun-Nan regions of China, *Bull. Seism. Soc. Am.,* **74,** 1189-1207.

Chow, R. A. C., J. D. Fairhead, N. B. Henderson, and P. D. Marshall (1980). Magnitude and Q determinations in southern Africa using L_g wave amplitudes, *Geophys. J.,* **63,** 735-745.

Chun, K.-Y., G. F. West, R. J. Kokoski, and C. Samson (1987). A novel technique for measuring L_g attenuation - Results from Eastern Canada between 1 to 10 Hz, *Bull. Seism. Soc. Am.,* **77,** 398-419.

Chun, K.-Y., T. Zhu, and X. R. Shih (1992). Regional wave attenuation in Eurasia, *Scientific Report #2, Contract F29601-91-C-DB24,* Univ. of Toronto, Toronto, Ontario, Canada.

Dewey, J. W. and A. Grantz (1973). The Ghir earthquake of April 10, 1972 in the Zagros Mountains of Southern Iran: Seismotectonic aspects and some results of a field reconnaissance, *Bull. Seism. Soc. Am.,* **63,**, 2071-2090.

Dwyer, J. J., R. B. Herrmann, and O. W. Nuttli (1983). Spatial attenuation of the L_g wave in the central United States. *Bull. Seism. Soc. Am.,* **73,** 781-796.

Ewing, M., J. M. Jardetzky, and F. Press (1957). *Elastic Waves in Layered Media,* 358 pages, McGraw-Hill, New York.

Given, H. (1991). Heterogeneous propagation and blockage of L_g in the Caspian Sea --- Caucasus Mountain area of the U.S.S.R., *Special Report PL-TR-91-2208, Proceeding of 13th PL/DARPA Seismic Research Symposium,* (J. F. Lewkowicz and J. M. McPhetres eds.) (8-10 October, 1991, Keystone, CO.), Phillips Laboratory, Hanscom Air Force Base, MA. **(ADA241325)**

Goncz, J. H., W. C. Dean, Z. A. Der, A. C. Lees, K. L. McLaughlin, T. W. McElfresh, and M. E. Marshall (1987). Propagation and excitation of L_g, S_n, and P-P_n waves from Eastern United States earthquakes by regression analysis of RSTN data, *Report TGAL-86-7,* Teledyne Geotech, Alexandria, Virginia.

Gupta, I. N., J. A. Burnetti, T. W. McElfresh, D. H. von Seggern, and R. A. Wagner (1983). Lateral variations in attenuation of ground motion in the eastern United States based on propagation of L_g, *NUREG/CR-3555,* U. S. Nuclear Regulatory Commission, Washington, D.C.

Gupta, I. N. and K. L. McLaughlin (1987). Attenuation of ground motion in the Eastern United States, *Bull. Seism. Soc. Am.,* **77,** 366-383.

Hasegawa, H. S. (1985). Attenuation of L_g waves in the Canadian Shield, *Bull. Seism. Soc. Am.,* **75,** 1569-1582.

Hedayati, A., J. L. Brander, and M. Berberian (1976). Microearthquake survey of Tehran region, Iran, *Bull. Seism. Soc. Am.,* **66,** 1713-1725.

Herrmann, R. B. (1980). *Q* estimates using the coda of local earthquakes, *Bull. Seism. Soc. Am.,* **70,** 447-468.

Horner, R. B., A. E. Stevens, H. S. Hasegawa, and G. LeBlanc (1978). Focal parameters of the July 12, 1975, Maniwaki, Quebec, earthquake - an example of intraplate seismicity in eastern Canada, *Bull. Seism. Soc. Am.,* **68,** 619-640.

Jackson, J. and D. McKenzie (1984). Active tectonics of the Alpine-Himalayan belt between western Turkey and Pakistan, *Geophys. J. R. astr. Soc.,* **77,** 185-264.

Jackson, J. and D. McKenzie (1988). The relationship between plate motions and seismic moment tensors, and the rates of active deformation in the Mediterranean and Middle East, *Geophys. J.,* **93,** 45-73.

Jih, R.-S. (1992). Simultaneous inversion of explosion size and path attenuation parameter with crustal phases, *Report TGAL-92-11,* Teledyne Geotech, Alexandria, VA.

Jih, R.-S. and C. S. Lynnes (1992). Re-examination of regional L_g *Q* variation in Iranian Plateau, in *Special Report PL-TR-92-2210, Proceedings of 14th Annual PL/DARPA Seismic Research Symposium, 16-18 Sept 1992, Tucson, AZ.* (J. F. Lewkowicz and J. M. McPhetres eds.), Phillips Laboratory, Hanscom Air Force Base, MA. **(ADA256711)**

Jih, R.-S. and R. A. Wagner (1992a). Path-corrected body-wave magnitudes and yield estimates of Novaya Zemlya explosions, *Report PL-TR-92-2042,* Phillips Laboratory, Hanscom Air Force Base, MA. **(ADA251240)**

Jih, R.-S. and R. A. Wagner (1992b). Path-corrected body-wave magnitudes and yield estimates of Semipalatinsk explosions, *Report TGAL-92-05,* Teledyne Geotech, Alexandria, VA.

Kadinsky-Cade, K., M. Barazangi, J. Oliver, and B. L. Isacks (1981). Lateral variations of high-frequency seismic wave propagation at regional distances across the Turkish and Iranian Plateaus, *J. Geophys. Res.,* **86,** 9377-9396.

Kennett, B. L. N., S. Gregersen, S. Mykkeltveit, and R. Newmark (1985). Mapping of crustal heterogeneity in the North Sea basin via the propagation of L_g waves, *Geophys. J.,* **83,** 299-306.

Leith, W. (1992). Geological factors affecting seismic monitoring in countries of nuclear proliferation concern, *Seismo. Res. Lett.,* **63,** 26.

Levshin, A. L., T. B. Yanovskaya, A. V. Lander, B. G. Bukchin, M. P. Barmin, L. I. Ratnikova, and E. N. Its (1989) (Keilis-Borok ed.). *Seismic Surface Waves in a Laterally Inhomogeneous Earth,* Kluwer Academic Publishers, Dordrecht/Boston/London, 293 pages.

Lynnes, C. S. and R. Baumstark (1991). Phase and spectral ratio discrimination in North America, *Report PL-TR-91-2212(II) (TGAL-91-06),* Phillips Laboratory, Hanscom Air Force Base, MA. **(ADA246673)**

Lynnes, C. S., R. Baumstark, R. K. Cessaro and W. W. Chan (1990). P_g / L_g discrimination in the western United States, *Report GL-TR-90-0167 (TGAL-90-05),* Geophysics Laboratory, Hanscom Air Force Base, MA. **(ADA226819)**

Lynnes, C. S. and R.-S. Jih (1991). Regional phase propagation in Central Asia, in *Special Report PL-TR-91-2208, Proceeding of 13th PL/DARPA Seismic Research Symposium, 8-10 October, 1991, Keystone, CO.* (J. F. Lewkowicz and J. M. McPhetres eds.), Phillips Laboratory, Hanscom Air Force Base, MA. **(ADA241325)**

McEvilly, T. V. and R. Razani (1971). A preliminary report: The Qir, Iran earthquake of April 10,1972, *Bull. Seism. Soc. Am.,* **63,** 339-354.

McKenzie, D. (1972). Active tectonics in the Mediterranean region, *Geophys. J. R. astr. Soc.,* **30,** 109-185.

Mechler, P., Nicolas, M. and A. Chaouch (1980). Seismic crustal and subcrustal phase propagation, *Final report for the AFOSR,* Laboratoire de Geophysique Appliquee, Universite Pierre et Marie Curie, Paris, France.

Mitchell, B. J. (1979). Higher mode attenuation in the Middle East --- Iran to Turkey, *Semiannual report of AFOSR contract F49620-79-C-0025,* Saint Louis University, Saint Louis, MO.

Mitchell, B. J. (1981). Regional variations and frequency dependence of Q_β in the crust of the North America, *Bull. Seism. Soc. Am.,* **71,** 1531-1538.

Mitchell, B. J. and H. J. Hwang (1987). Effect of low Q sediments and crustal Q on Lg attenuation in the United States, *Bull. Seism. Soc. Am.,* **77,** 1197-1210.

Ni, J., and M. Barazangi (1983). High-frequency seismic wave propagation beneath the Indian Shield, Himalayan Arc, Tibetan Plateau, and surrounding regions: high uppermost mantle velocities and efficient S_n propagation beneath Tibet, *Geophys. J. R. astr. Soc.,* **72,** 665-689.

Niazi, M. (1980). Microearthquakes and crustal structure off the Markran coast of Iran, *Geophys. Res. Lett.,* **7,** 297-300.

Nowroozi, A. (1971). Seismotectonics of the Persian Plateau, eastern Turkey, Caucasus, and Hindu-Kush regions, *Bull. Seism. Soc. Am.,* **61,** 315-341.

Nowroozi, A. (1972). Focal mechanisms of earthquakes in Persia, Turkey, West Pakistan, and Afganistan and plate tectonics of the Middle East, *Bull. Seism. Soc. Am.,* **62,** 823-850.

Nowroozi, A. (1976). Seismotectonic provinces of the Persian Plateau, *Bull. Seism. Soc. Am.,* **66,** 1249-1276.

Nuttli, O. W. (1973). Seismic wave attenuation and magnitude relations for eastern North America, *J. Geophys. Res.,* **78,** 876-885.

Nuttli, O. W. (1980). The excitation and attenuation of seismic crustal phases in Iran, *Bull. Seism. Soc. Am.,* **70,** 469-485.

Nuttli, O. W. (1981). On the attenuation of L_g waves in Western and Central Asia and their use as a discriminant between earthquakes and explosions, *Bull. Seism. Soc. Am.,* **71,** 249-261.

Nuttli, O. W. (1986). Yield estimates of Nevada Test Site explosions obtained from seismic L_g waves, *J. Geophys. Res.*, **91,** 2137-2151.

Pomeroy, P. W., W. J. Best, and T. V. McEvilly (1982). Test ban treaty verification with regional data -- a review, *Bull. Seism. Soc. Am.,* **72,** S89-S129.

Pulli, J. (1984). Attenuation of coda waves in New England, *Bull. Seism. Soc. Am.,* **74,** 1149-1166.

Quinttmeyer, R. C. and K. H. Jacob (1979). Historical and modern seismicity of Pakistan, Afghanistan, northwestern India, and southeastern Iran, *Bull. Seism. Soc. Am.,* **69,** 773-823.

Raoof, M. M. and O. W. Nuttli (1985). Attenuation of high-frequency earthquake waves in South America, *Pure and Applied Geophysics,* **122,** 619-644.

Rowshandel, B., S. Nemat-Nasser, and R. B. Cortis (1981). A comparative seismic hazard study for Azerbaijan province in Iran, *Bull. Seism. Soc. Am.,* **71,** 335-360.

Ruzaikan, A. I., I. L. Nersesov, V. I. Khalturin, and P. Molnar (1977). Propagation of L_g and lateral variation in crustal structure in Asia, *J. Geophys. Res.,* **82,** 307-316.

Seber, D. and B. J. Mitchell (1991). Attenuation of surface waves across the Arabian Peninsula, *Report PL-TR-91-2286,* Phillips Laboratory, Hanscom Air Force Base, MA. **(ADA251590)**

Singh, S. and R. B. Herrmann (1983). Regionalization of crustal coda Q in the continental United States, *J. Geophys. Res.,* **88,** 527-538.

Shin, T.-C. (1985). L_g and coda wave studies of Eastern Canada, *Ph. D. Dissertation,* Saint Louis University, St. Louis, Missouri, 185 pp.

Shin, T.-C. and R. B. Herrmann (1987). L_g attenuation and source studies using 1982 Miramichi data, *Bull. Seism. Soc. Am.* **77,** 384-397.

Street, R. L. (1976). Scaling northeastern United States/southern Canadian earthquakes by their L_g waves, *Bull. Seism. Soc. Am.,* **66,** 1525-1537.

Wallace, T. C. (1991). The effects of crustal structure on spectral discriminates, in *Special Report PL-TR-91-2208, Proceeding of 13th PL/DARPA Seismic Research Symposium, 8-10 October, 1991, Keystone, CO.* (J. F. Lewkowicz and J. M. McPhetres eds.), Phillips Laboratory, Hanscom Air Force Base, MA. **(ADA241325)**

Xie, J. and B. J. Mitchell (1990). A back-projection method for imaging large-scale lateral variations of L_g coda Q with application to continental Africa, *Geophys. J.,* **100,** 161-181.

Xie, J. and B. J. Mitchell (1990). Attenuation of multiphase surface waves in the Basin and Range provinces, Part I: L_g and L_g coda, *Geophys. J.,* **102,** 121-137.

Xie, J. and B. J. Mitchell (1991). L_g coda-Q variation across Eurasia, Chapter 3 in *Report PL-TR-91-2286,* Phillips Laboratory, Hanscom Air Force Base, MA. **(ADA251590)**

(THIS PAGE INTENTIONALLY LEFT BLANK)

STUDIES OF SEISMIC WAVE PROPAGATION IN EURASIA

Rong-Song Jih
Teledyne Geotech
314 Montgomery Street
Alexandria, VA 22314

Christopher S. Lynnes
Hughes STX
7601 Ora Glen Drive, Suite 300
Greenbelt, MD 20770

1. CONTRACT NO.: F19628-90-C-0158 (16 Aug 1990 - 15 Dec 1992)

2. MOST IMPORTANT SCIENTIFIC RESULTS

Under this Air Force-funded contract, we have been conducting both theoretical and observational studies covering a wide spectrum of topics directly related to monitoring the compliance of both the Threshold Test Ban Treaty [TTBT] and the Non-Proliferation Treaty [NPT]. Each of the following paragraphs summarizes a paper that has been or will be presented/published. The investigator who performed the specific task is also identified.

2.1 ISC Travel Time Inversion in the Garm Region, Central Asia[1] (Lynnes)

The propagation of regional phases is still problematic: amplitudes and even the observability of phases can be highly variable. This has important implications for the application and efficacy of earthquake/explosion discriminants and event size estimation. At least some of this variation is likely due to the effects of lateral heterogeneity, particularly in the waveguides and near the boundaries along which regional phases such as P_g , P_n , S_n , and L_g propagate. The effects of lateral heterogeneity on regional phase propagation can be modeled using finite-difference methods.

In order to employ these methods, a realistic velocity model is required. Block inversion of travel times is a well-established technique for deriving laterally heterogeneous velocity structures. In order to simplify the problem and improve ray coverage, a two-dimensional geometry is sought: the high seismicity rate along the great circle arc between the IRIS station GAR and and the CDSN station WMQ provides such an opportunity. Travel times for regional phases are used to derive a spherically symmetric structure for the crust and upper mantle in this region. This model is then starting model for a two-dimensional velocity inversion in the vertical plane.

[1]Reported in Semi-annual R&D Status Reports #1 and #2 dated 14 February and 19 August, 1991, respectively. See also Section I of this report.

2.2 Path Effects on Body-wave Amplitudes of Novaya Zemlya Explosions[2] (Jih)

The standard procedure used in estimating the source size of underground nuclear explosions using m_b measurements has been to separate the station terms from the network-averaged source terms. The station terms thus derived actually reflect the combination of the path effect and the station effect, when only those events in a close proximity are utilized. If worldwide explosions are used in the inversion, then the path effect tends to be averaged out at each station. In either case, the effect due to the propagation path alone would not be obvious.

The major research goal of this contract is to improve our fundamental understanding of the seismic wave propagation in Eurasia. To achieve this goal, we further decompose the station amplification effect with a joint inversion scheme that simultaneously determines the seismic source size, the path terms, and the receiver terms. Short-period P-wave amplitudes of 217 worldwide underground nuclear explosions, including 28 blasts from Novaya Zemlya, recorded at 118 WWSSN stations have been used in one single inversion to isolate the propagation complexities affecting the P-wave amplitudes. For all 28 Novaya Zemlya events in our WWSSN database, the new m_b factoring procedure provides more stable m_b measurements across the whole recording network with a reduction in the fluctuational variation by a factor of up to 3. A typical reduction factor in the variation is about 2.0, and the the worst case is 1.4.

The inferred path terms are then compared against the travel-time residuals to characterize the propagation paths. Our result indicates that paths from the northern test site in Novaya Zemlya to stations in North America have systematically faster arrivals and smaller amplitudes, suggesting a profound defocusing effect on the first arrivals; while stations in Ireland, Scotland, Spain, Bangladesh, northern India, Pakistan, Korea, and Kenya report slow arrivals and large amplitudes, suggesting a focusing effect. Amplitudes for paths to Greenland, Iceland, Alaska, Turkey, Germany, Luzon, Zimbabwe, Italy, Pueto Rico, Ethiopia, and Hawaii, however, seem to be controlled by the anelastic attenuation with slow rays also associated with small amplitudes, and fast rays associated with large amplitudes. A strong correlation between $P-$wave amplitude and L_g detection at teleseismic distance is also observed.

---

[2]Reported in Semi-annual R&D Status Report #3 dated 16 February, 1992, and Scientific Report #1, *PL-TR-92-2042*.

2.3 Yield Estimates of Novaya Zemlya Explosions: Preliminary Result[3] (Jih)

As a byproduct of the study described in Section 2.2, we have derived the yield estimates of Novaya Zemlya explosions based on the path-corrected m_b values. Assuming the basic coupling and the mantle condition at Novaya Zemlya are comparable to those at Eastern Kazakhstan, the m_b bias relative to NTS at 50 KT level using the path-corrected m_b (P_{max}) values is inferred as 0.25 and 0.36 magnitude unit for Novaya Zemlya and Semipalatinsk, respectively. The m_b (P_{max}) bias of 0.11 between Semipalatinsk and Novaya Zemlya could be largely due to the difference in *pP* interference between these two test sites (rather than the seismic coupling). The relative source size determined by Burger *et al.* (1986) and the theoretical $\log(\Psi_\infty)$:yield scaling are combined to extrapolate our m_b scaling to the higher end. The resulting yield estimates of Novaya Zemlya explosions range from 2 to 2100 KT, with peak values at 550 KT and 65 KT for events before and after 1976, respectively, which are in reasonable agreement with those in previous studies.

Also included in the Annual Scientific Report No. 1 is a complete listing of path-corrected m_b values and yield estimates of Semipalatinsk explosions which are used as our baseline in calibrating Novaya Zemlya explosions. First motion of the initial short-period *P* waves appears to be a very favorable source measure for explosions fired in hard rock sites underlain by the stable mantle (such as Semipalatinsk).

2.4 Regional Lg Q Variation in the Iranian Plateau Revisited[4] (Jih)

We examined a general procedure which incorporates the independently-derived information of localized path effects into the magnitude determination. The goal of this exercise is to quantify the bias in the seismic magnitude (such as $m_b(L_g)$) that would be inherent in a scheme without fully coupling the regional propagational characteristics into the magnitude determination procedure. Iran was chosen as a test case in this study because of the growing nuclear proliferation concern in the Middle East.

A tentative zoning partitioning Iranian Plateau into six regions (*viz.*, the Zagros Range, the Lut Block, East Iran Range, Central Iran Range, the Elburz/Caspian area, and the Great Kavir/Esfaphan/Rezaiyeh region) has been used in our block inversion to reveal the spatial pattern of the L_g attenuation parameter, Q. We used 109 observations recorded at 3 WWSSN stations in Iran (MSH, TAB, and SHI) for which the γ was readily measured by Nuttli

[3]Reported in Semi-annual R&D Status Report #3 dated 16 February, 1992, and Scientific Report #1, *PL-TR-92-2042*.

[4]Reported in Semi-annual R&D Status Report #4 dated 14 August, 1992. See also Section II of this report.

(1980). The weighted average γ of these paths is 0.0044 km^{-1}, very close to the 0.0048 for coastal California derived by Herrmann (1980). It is also in agreement with the L_g coda Q map recently compiled by Xie and Mitchell (1992) for Eurasia. In our inversion with a more detailed regionalization, both the Zagros Range and the Lut Block show a large γ of 0.005 km^{-1}, roughly corresponding to a Q of 181±12 and 183±18, respectively. The Kopet Dagh, Shahrud Doruneh, and the Qom region also seem to have a Q slightly smaller than the average. On the other hand, the Elburz Province and central Iran have a Q of about 250 for 1 Hz L_g waves, which could be the highest Q value in Iran.

Although the whole Iranian Plateau can be briefly described as a region of very low Q, applying a simple averaged attenuation coefficient (Q) for the whole plateau would be inappropriate. The regional variation of the anelastic attenuation parameter is significant enough that it must be taken into account in calibrating each monitoring station for a reliable magnitude scale in monitoring possible clandestine tests from a vast area. Unless this has been done, adding more stations/arrays to the monitoring network may not provide substantial improvement in reducing the error in the network-averaged magnitude based on regional phases. In fact, the bias in $m_b(L_g)$ would be much smaller if the magnitude was solely based on the nearest station alone (as compared to using a network of sparse stations for simple averaging). This situation is very different from that of monitoring a specific nuclear test site for which the empirical site-dependent correction term can be applied afterwards to the station magnitudes even when the path Qs are not fully known in advance.

2.5 Theoretical Investigation of Ripple-fired Explosions[5] (Jih)

A major issue for the Non-Proliferation Treaty is the discrimination of large chemical explosions from possible clandestine or small nuclear tests. Unless discrimination is possible, the numerous mining blasts could give ample opportunity for concealing clandestine tests. Rippled-fired explosions are commonly used for fragmenting rocks during quarry and open-pit mining. The periodicity inherent in the ripple firing could produce a seismic reinforcement at the frequency of the delay between shots or rows. Since ripple firing is essentially a sequence of single explosions arranged and fired using a series of time-delayed detonations between adjacent shot holes or rows of shot holes, it has been suggested that the convolution of a single explosion with a comb function of variable spacing and variable amplitude can be used to study the distinctive signature of ripple firing (Stump, 1988; Smith, 1989). Baumgardt and Ziegler (1988) delicately demonstrated that the incoherent array-stack spectra can be

[5]Reported in Semi-annual R&D Status Report #4 dated 14 August 1992.

used to identify some multiple shots recorded at NORSAR. By superpositioning the waveform due to a single shot with proper time delay, they were able to model the source multiplicity under the assumption that the spatial spreading of the shots are negligible with respect to the traveling distance.

There are, however, wave excitation characteristics of ripple-fired explosions which are not predicted by such spectral or waveform superposition approaches. Figure 1 of our 4th semi-annual R&D status report shows the vertical component of the displacement wave field of 7 ripple-fired explosions detonated with a *rupture velocity* of 2.5 km/s in a granitic half space. Neither R_g nor the S* was emitted in the single explosion case using the same shot depth. However, a very clear R_g is excited in the forward direction for the ripple firing. In fact, one of the standard industrial practices in reducing potential damage caused by ground vibration is to detonate ripple shots in a direction away from the buildings (Dick *et al.*, 1983). An immediate implication of this exercise on the discrimination problem is that the lack of R_g is not necessarily indicative of deep sources. Furthermore, although path effects such as anelastic attenuation and scattering by shallow heterogeneity and topography in the upper crust can reduce R_g significantly as demonstrated by Jih *et al.* (1988) and McLaughlin and Jih (1986, 1987), the reported lack of R_g in many seismograms from known quarry blasts could also be due to the intrinsic source effect (such as the shooting pattern) rather than the path effects.

Several previous theoretical studies with spectral superposition approach (*e.g.*, Smith, 1989; Greenhalgh, 1980) suggest that for ripple firings with simple configurations, the spectrum will be reinforced at every $1/\Delta t$ Hz, where the Δt is the delay time between the shots. However, our numerical experiments indicate that even with a very simple linearly distributed shot array in the half space, the frequencies at which the amplitude reinforcement could occur also depend on the relative azimuth angle and take-off angle with respect to the rupture direction. Figure 2 of our 4th semi-annual R&D status report gives the spectral ratios of *P*-wave synthetics to that due to a single explosion. It is clear that reinforcement does occur at exactly every 50 Hz along the orthogonal direction, consistent with Smith's prediction (1987, 1989). For other directions, however, the frequency at which the enhancement would occur is clearly off due to the *Doppler Effect.* This phenomenon suggests that the shift of the spectral reinforcement, whenever observable, could be used as a simple discriminant between multiple explosions and a single shot. It could also provide an alternative explanation of why the spectral reinforcement was not observed at the expected frequency at RSON for the mining blast C detonated at Mesabi Range, August 6 1986 (Smith, 1989). Kim *et al.* (1991) report that

seismograms from the same quarry recorded at the same station could have distinct spectral characteristics. They attribute this phenomenon to the considerable fluctuation in delay times and sub-charge sizes. The numerical modeling study we conducted provides another possible explanation, however.

2.6 Lop Nor Explosion of 21 May 1992 as Observed at ANP (Anpu, WWSSN), Taiwan (Jih)

The "megaton"-level explosion detonated on 21 May 1992 at the test site between Lop Nor and Bosten Lake, Xinjiang, is believed to be the largest Chinese underground nuclear test conducted so far. The raw body-wave magnitudes (*viz.*, log(A/T) + B(Δ)) measured at WWSSN station ANP (Anpu, 121.517°E, 25.183°N, Δ=3523km) are 5.72, 6.17, and 6.43, based on the first motion (zero-to-peak or P_a), the "b" phase (first peak-to-first trough or P_b), and the largest peak-to-peak (P_{max}) amplitudes, respectively. Applying the empirical station correction of 0.143 magnitude unit [m.u.] along with the path correction of -0.045 m.u. derived by Jih and Wagner (1992a) to bring the station recordings at ANP in alignment with the optimal worldwide network average, the final station m_b values at ANP are set at 5.82 (P_a), 6.27 (P_b), and 6.52 (P_{max}), respectively. Since there is no evidence of a low velocity zone [LVZ] in the area of eastern Tien Shan Mountains or the test site (Matzko, 1992), it would seem reasonable that the upper-mantle conditions at Lop Nor test site are very similar to those at Eastern Kazakh where the major nuclear test sites of the former Soviet Union are located. As a result, the magnitude-yield calibration curve derived from the P_a phases of Eastern Kazakh explosions (*cf.* Jih and Wagner, 1992a,b) could be adequate for Lop Nor explosions as well. The calibration curves for P_b and P_{max} phases can then be inferred from the empirical P_b -P_a and P_{max}-P_a regressions, respectively. Under the assumption that the source coupling as well as the anelastic attenuation at Lop Nor test site are comparable to those at Eastern Kazakh, and further that the corner-frequency effect is negligible, the yield of 21 May 1992 explosion is estimated as 350 KT based on the m_b values measured at ANP alone. If we assume that Lop Nor area has a t* intermediate between those at Nevada test site (U.S.A.) and Eastern Kazakh, then our yield estimate would become 550 KT instead. This seems, however, very unlikely as the alternative assumption lacks geophysical support. The news media report that the nuclear device was emplaced in a shaft somewhat over 900 meters deep which, if correct, would suggest a yield most likely in the range of 400-480 KT and no more than 550 KT. Thus 350 KT and 550 KT can be regarded as the lower and upper bounds, respectively, of our preliminary yield estimate.

3. REPORTS AND PRESENTATIONS DELIVERED

(1991) Regional phase propagation in Central Asia, in *Special Report PL-TR-91-2208, Proceedings of 13th DARPA/PL Seismic Research Symposium, 8-10 Oct 1991, Keystone, CO.* (Eds J. Lewkowicz and J. McPhetres), Phillips Laboratory, Hanscom Air Force Base, MA. **(ADA241325)**

(1992) Path-corrected body-wave magnitudes and yield estimates of Novaya Zemlya explosions, *Report PL-TR-92-2042 (=TGAL-91-09), Scientific Report #1,* Phillips Laboratory, Hanscom Air Force Base, MA. **(ADA251240).**

(1992) Path effects on body-wave magnitudes of Novaya Zemlya explosions, *EOS, Trans. Am. Geophys. Union,* **73-14**, 209.

(1992) Yield estimates of Novaya Zemlya explosions based on path-corrected short-period body-wave amplitudes, *EOS, Trans. Am. Geophys. Union,* **73-25**, 64.

(1992) Re-examination of regional L_g Q variation in Iranian Plateau, in *Special Report PL-TR-92-2210, Proceedings of 14th DARPA/PL Seismic Research Symposium, 16-18 Sept 1992, Tucson, AZ.* (Eds J. Lewkowicz and J. McPhetres), Phillips Laboratory, Hanscom Air Force Base, MA. **(ADA256711)**

(1992) Simultaneous inversion of explosion size and path attenuation coefficient with crustal phases (submitted for publication).[6]

(1992) Lop Nor explosion of 21 May 1992 as observed at ANP (Anpu, WWSSN), Taiwan, *EOS, Trans. Am. Geophys. Union,* **73-43**, 359.

(1993) Studies of regional phase propagation in Eurasia, *Report PL-TR-93-2003 (=TGAL-93-01), Final Report,* Phillips Laboratory, Hanscom Air Force Base, MA.

---

[6]Jointly supported under PL contracts F19628-90-C-0158 and F29601-91-C-DB23.

(THIS PAGE INTENTIONALLY LEFT BLANK)

Prof. Thomas Ahrens
Seismological Lab, 252-21
Division of Geological & Planetary Sciences
California Institute of Technology
Pasadena, CA 91125

Prof. Keiiti Aki
Center for Earth Sciences
University of Southern California
University Park
Los Angeles, CA 90089-0741

Prof. Shelton Alexander
Geosciences Department
403 Deike Building
The Pennsylvania State University
University Park, PA 16802

Dr. Ralph Alewine, III
DARPA/NMRO
3701 North Fairfax Drive
Arlington, VA 22203-1714

Prof. Charles B. Archambeau
CIRES
University of Colorado
Boulder, CO 80309

Dr. Thomas C. Bache, Jr.
Science Applications Int'l Corp.
10260 Campus Point Drive
San Diego, CA 92121 (2 copies)

Prof. Muawia Barazangi
Institute for the Study of the Continent
Cornell University
Ithaca, NY 14853

Dr. Jeff Barker
Department of Geological Sciences
State University of New York
at Binghamton
Vestal, NY 13901

Dr. Douglas R. Baumgardt
ENSCO, Inc
5400 Port Royal Road
Springfield, VA 22151-2388

Dr. Susan Peck
Department of Geosciences
Building #77
University of Arizona
Tuscon, AZ 85721

Dr. T.J. Bennett
S CUBED
A Division of Maxwell Laboratories
11800 Sunrise Valley Drive, Suite 1212
Reston, VA 22091

Dr. Robert Blandford
AFTAC/TT, Center for Seismic Studies
1300 North 17th Street
Suite 1450
Arlington, VA 22209-2308

Dr. Stephen Bratt
Center for Seismic Studies
1300 North 17th Street
Suite 1450
Arlington, VA 22209-2308

Dr. Lawrence Burdick
Woodward Clyde Consultants
566 El Dorado Street
Pasadena, CA 91109-3245

Dr. Robert Burridge
Schlumberger-Doll Research Center
Old Quarry Road
Ridgefield, CT 06877

Dr. Jerry Carter
Center for Seismic Studies
1300 North 17th Street
Suite 1450
Arlington, VA 22209-2308

Dr. Eric Chael
Division 9241
Sandia Laboratory
Albuquerque, NM 87185

Dr. Martin Chapman
Department of Geological Sciences
Virginia Polytechnical Institute
21044 Derring Hall
Blacksburg, VA 24061

Prof. Vernon F. Cormier
Department of Geology & Geophysics
U-45, Room 207
University of Connecticut
Storrs, CT 06268

Prof. Steven Day
Department of Geological Sciences
San Diego State University
San Diego, CA 92182

Marvin Denny
U.S. Department of Energy
Office of Arms Control
Washington, DC 20585

Dr. Zoltan Der
ENSCO, Inc.
5400 Port Royal Road
Springfield, VA 22151-2388

Prof. Adam Dziewonski
Hoffman Laboratory, Harvard University
Dept. of Earth Atmos. & Planetary Sciences
20 Oxford Street
Cambridge, MA 02138

Prof. John Ebel
Department of Geology & Geophysics
Boston College
Chestnut Hill, MA 02167

Eric Fielding
SNEE Hall
INSTOC
Cornell University
Ithaca, NY 14853

Dr. Mark D. Fisk
Mission Research Corporation
735 State Street
P.O. Drawer 719
Santa Barbara, CA 93102

Prof Stanley Flatte
Applied Sciences Building
University of California, Santa Cruz
Santa Cruz, CA 95064

Dr. John Foley
NER-Geo Sciences
1100 Crown Colony Drive
Quincy, MA 02169

Prof. Donald Forsyth
Department of Geological Sciences
Brown University
Providence, RI 02912

Dr. Art Frankel
U.S. Geological Survey
922 National Center
Reston, VA 22092

Dr. Cliff Frohlich
Institute of Geophysics
8701 North Mopac
Austin, TX 78759

Dr. Holly Given
IGPP, A-025
Scripps Institute of Oceanography
University of California, San Diego
La Jolla, CA 92093

Dr. Jeffrey W. Given
SAIC
10260 Campus Point Drive
San Diego, CA 92121

Dr. Dale Glover
Defense Intelligence Agency
ATTN: ODT-1B
Washington, DC 20301

Dr. Indra Gupta
Teledyne Geotech
314 Montgomery Street
Alexanderia, VA 22314

Dan N. Hagedon
Pacific Northwest Laboratories
Battelle Boulevard
Richland, WA 99352

Dr. James Hannon
Lawrence Livermore National Laboratory
P.O. Box 808
L-205
Livermore, CA 94550

Dr. Roger Hansen
HQ AFTAC/TTR
Patrick AFB, FL 32925-6001

Prof. David G. Harkrider
Seismological Laboratory
Division of Geological & Planetary Sciences
California Institute of Technology
Pasadena, CA 91125

Prof. Danny Harvey
CIRES
University of Colorado
Boulder, CO 80309

Prof. Donald V. Helmberger
Seismological Laboratory
Division of Geological & Planetary Sciences
California Institute of Technology
Pasadena, CA 91125

Prof. Eugene Herrin
Institute for the Study of Earth and Man
Geophysical Laboratory
Southern Methodist University
Dallas, TX 75275

Prof. Robert B. Herrmann
Department of Earth & Atmospheric Sciences
St. Louis University
St. Louis, MO 63156

Prof. Lane R. Johnson
Seismographic Station
University of California
Berkeley, CA 94720

Prof. Thomas H. Jordan
Department of Earth, Atmospheric &
Planetary Sciences
Massachusetts Institute of Technology
Cambridge, MA 02139

Prof. Alan Kafka
Department of Geology & Geophysics
Boston College
Chestnut Hill, MA 02167

Robert C. Kemerait
ENSCO, Inc.
445 Pineda Court
Melbourne, FL 32940

Dr. Karl Koch
Institute for the Study of Earth and Man
Geophysical Laboratory
Southern Methodist University
Dallas, Tx 75275

Dr. Max Koontz
U.S. Dept. of Energy/DP 5
Forrestal Building
1000 Independence Avenue
Washington, DC 20585

Dr. Richard LaCoss
MIT Lincoln Laboratory, M-200B
P.O. Box 73
Lexington, MA 02173-0073

Dr. Fred K. Lamb
University of Illinois at Urbana-Champaign
Department of Physics
1110 West Green Street
Urbana, IL 61801

Prof. Charles A. Langston
Geosciences Department
403 Deike Building
The Pennsylvania State University
University Park, PA 16802

Jim Lawson, Chief Geophysicist
Oklahoma Geological Survey
Oklahoma Geophysical Observatory
P.O. Box 8
Leonard, OK 74043-0008

Prof. Thorne Lay
Institute of Tectonics
Earth Science Board
University of California, Santa Cruz
Santa Cruz, CA 95064

Dr. William Leith
U.S. Geological Survey
Mail Stop 928
Reston, VA 22092

Mr. James F. Lewkowicz
Phillips Laboratory/GPEH
Hanscom AFB, MA 01731-5000(2 copies)

Mr. Alfred Lieberman
ACDA/VI-OA State Department Building
Room 5726
320-21st Street, NW
Washington, DC 20451

Prof. L. Timothy Long
School of Geophysical Sciences
Georgia Institute of Technology
Atlanta, GA 30332

Dr. Randolph Martin, III
New England Research, Inc.
76 Olcott Drive
White River Junction, VT 05001

Dr. Robert Masse
Denver Federal Building
Box 25046, Mail Stop 967
Denver, CO 80225

Dr. Gary McCartor
Department of Physics
Southern Methodist University
Dallas, TX 75275

Prof. Thomas V. McEvilly
Seismographic Station
University of California
Berkeley, CA 94720

Dr. Art McGarr
U.S. Geological Survey
Mail Stop 977
U.S. Geological Survey
Menlo Park, CA 94025

Dr. Keith L. McLaughlin
S-CUBED
A Division of Maxwell Laboratory
P.O. Box 1620
La Jolla, CA 92038-1620

Stephen Miller & Dr. Alexander Florence
SRI International
333 Ravenswood Avenue
Box AF 116
Menlo Park, CA 94025-3493

Prof. Bernard Minster
IGPP, A-025
Scripps Institute of Oceanography
University of California, San Diego
La Jolla, CA 92093

Prof. Brian J. Mitchell
Department of Earth & Atmospheric Sciences
St. Louis University
St. Louis, MO 63156

Mr. Jack Murphy
S-CUBED
A Division of Maxwell Laboratory
11800 Sunrise Valley Drive, Suite 1212
Reston, VA 22091 (2 Copies)

Dr. Keith K. Nakanishi
Lawrence Livermore National Laboratory
L-025
P.O. Box 808
Livermore, CA 94550

Dr. Carl Newton
Los Alamos National Laboratory
P.O. Box 1663
Mail Stop C335, Group ESS-3
Los Alamos, NM 87545

Dr. Bao Nguyen
HQ AFTAC/TTR
Patrick AFB, FL 32925-6001

Prof. John A. Orcutt
IGPP, A-025
Scripps Institute of Oceanography
University of California, San Diego
La Jolla, CA 92093

Prof. Jeffrey Park
Kline Geology Laboratory
P.O. Box 6666
New Haven, CT 06511-8130

Dr. Howard Patton
Lawrence Livermore National Laboratory
L-025
P.O. Box 808
Livermore, CA 94550

Dr. Frank Pilotte
HQ AFTAC/TT
Patrick AFB, FL 32925-6001

Dr. Jay J. Pulli
Radix Systems, Inc.
2 Taft Court, Suite 203
Rockville, MD 20850

Dr. Robert Reinke
ATTN: FCTVTD
Field Command
Defense Nuclear Agency
Kirtland AFB, NM 87115

Prof. Paul G. Richards
Lamont-Doherty Geological Observatory
of Columbia University
Palisades, NY 10964

Mr. Wilmer Rivers
Teledyne Geotech
314 Montgomery Street
Alexandria, VA 22314

Dr George Rothe
HQ AFTAC/TTR
Patrick AFB, FL 32925-6001

Dr. Alan S. Ryall, Jr.
DARPA/NMRO
3701 North Fairfax Drive
Arlington, VA 22209-1714

Dr. Richard Sailor
TASC, Inc.
55 Walkers Brook Drive
Reading, MA 01867

Prof. Charles G. Sammis
Center for Earth Sciences
University of Southern California
University Park
Los Angeles, CA 90089-0741

Prof. Christopher H. Scholz
Lamont-Doherty Geological Observatory
of Columbia University
Palisades, NY 10964

Dr. Susan Schwartz
Institute of Tectonics
1156 High Street
Santa Cruz, CA 95064

Secretary of the Air Force
(SAFRD)
Washington, DC 20330

Office of the Secretary of Defense
DDR&E
Washington, DC 20330

Thomas J. Sereno, Jr.
Science Application Int'l Corp.
10260 Campus Point Drive
San Diego, CA 92121

Dr. Michael Shore
Defense Nuclear Agency/SPSS
6801 Telegraph Road
Alexandria, VA 22310

Dr. Robert Shumway
University of California Davis
Division of Statistics
Davis, CA 95616

Dr. Matthew Sibol
Virginia Tech
Seismological Observatory
4044 Derring Hall
Blacksburg, VA 24061-0420

Prof. David G. Simpson
IRIS, Inc.
1616 North Fort Myer Drive
Suite 1440
Arlington, VA 22209

Donald L. Springer
Lawrence Livermore National Laboratory
L-025
P.O. Box 808
Livermore, CA 94550

Dr. Jeffrey Stevens
S-CUBED
A Division of Maxwell Laboratory
P.O. Box 1620
La Jolla, CA 92038-1620

Lt. Col. Jim Stobie
ATTN: AFOSR/NL
Bolling AFB
Washington, DC 20332-6448

Prof. Brian Stump
Institute for the Study of Earth & Man
Geophysical Laboratory
Southern Methodist University
Dallas, TX 75275

Prof. Jeremiah Sullivan
University of Illinois at Urbana-Champaign
Department of Physics
1110 West Green Street
Urbana, IL 61801

Prof. L. Sykes
Lamont-Doherty Geological Observatory
of Columbia University
Palisades, NY 10964

Dr. David Taylor
ENSCO, Inc.
445 Pineda Court
Melbourne, FL 32940

Dr. Steven R. Taylor
Los Alamos National Laboratory
P.O. Box 1663
Mail Stop C335
Los Alamos, NM 87545

Prof. Clifford Thurber
University of Wisconsin-Madison
Department of Geology & Geophysics
1215 West Dayton Street
Madison, WS 53706

Prof. M. Nafi Toksoz
Earth Resources Lab
Massachusetts Institute of Technology
42 Carleton Street
Cambridge, MA 02142

Dr. Larry Turnbull
CIA-OSWR/NED
Washington, DC 20505

Dr. Gregory van der Vink
IRIS, Inc.
1616 North Fort Myer Drive
Suite 1050
Arlington, VA 22209

Dr. Karl Veith
EG&G
5211 Auth Road
Suite 240
Suitland, MD 20746

Prof. Terry C. Wallace
Department of Geosciences
Building #77
University of Arizona
Tuscon, AZ 85721

Dr. Thomas Weaver
Los Alamos National Laboratory
P.O. Box 1663
Mail Stop C335
Los Alamos, NM 87545

Dr. William Wortman
Mission Research Corporation
8560 Cinderbed Road
Suite 700
Newington, VA 22122

Prof. Francis T. Wu
Department of Geological Sciences
State University of New York
at Binghamton
Vestal, NY 13901

AFTAC/CA
(STINFO)
Patrick AFB, FL 32925-6001

DARPA/PM
3701 North Fairfax Drive
Arlington, VA 22203-1714

DARPA/RMO/RETRIEVAL
3701 North Fairfax Drive
Arlington, VA 22203-1714

DARPA/RMO/SECURITY OFFICE
3701 North Fairfax Drive
Arlington, VA 22203-1714

HQ DNA
ATTN: Technical Library
Washington, DC 20305

Defense Intelligence Agency
Directorate for Scientific & Technical Intelligence
ATTN: DTIB
Washington, DC 20340-6158

Defense Technical Information Center
Cameron Station
Alexandria, VA 22314 (2 Copies)

TACTEC
Battelle Memorial Institute
505 King Avenue
Columbus, OH 43201 (Final Report)

Phillips Laboratory
ATTN: XPG
Hanscom AFB, MA 01731-5000

Phillips Laboratory
ATTN: GPE
Hanscom AFB, MA 01731-5000

Phillips Laboratory
ATTN: TSML
Hanscom AFB, MA 01731-5000

Phillips Laboratory
ATTN: SUL
Kirtland, NM 87117 (2 copies)

Dr. Michel Bouchon
I.R.I.G.M.-B.P. 68
38402 St. Martin D'Heres
Cedex, FRANCE

Dr. Michel Campillo
Observatoire de Grenoble
I.R.I.G.M.-B.P. 53
38041 Grenoble, FRANCE

Dr. Kin Yip Chun
Geophysics Division
Physics Department
University of Toronto
Ontario, CANADA

Prof. Hans-Peter Harjes
Institute for Geophysic
Ruhr University/Bochum
P.O. Box 102148
4630 Bochum 1, GERMANY

Prof. Eystein Husebye
NTNF/NORSAR
P.O. Box 51
N-2007 Kjeller, NORWAY

David Jepsen
Acting Head, Nuclear Monitoring Section
Bureau of Mineral Resources
Geology and Geophysics
G.P.O. Box 378, Canberra, AUSTRALIA

Ms. Eva Johannisson
Senior Research Officer
FOA
S-172 90 Sundbyberg, SWEDEN

Dr. Peter Marshall
Procurement Executive
Ministry of Defense
Blacknest, Brimpton
Reading FG7-FRS, UNITED KINGDOM

Dr. Bernard Massinon, Dr. Pierre Mechler
Societe Radiomana
27 rue Claude Bernard
75005 Paris, FRANCE (2 Copies)

Dr. Svein Mykkeltveit
NTNT/NORSAR
P.O. Box 51
N-2007 Kjeller, NORWAY (3 Copies)

Prof. Keith Priestley
University of Cambridge
Bullard Labs, Dept. of Earth Sciences
Madingley Rise, Madingley Road
Cambridge CB3 OEZ, ENGLAND

Dr. Jorg Schlittenhardt
Federal Institute for Geosciences & Nat'l Res.
Postfach 510153
D-3000 Hannover 51, GERMANY

Dr. Johannes Schweitzer
Institute of Geophysics
Ruhr University/Bochum
P.O. Box 1102148
4360 Bochum 1, GERMANY

Trust & Verify
VERTIC
8 John Adam Street
LONDON WC2N 6EZ, ENGLAND